POLITECNICO DI TORINO
Repository ISTITUZIONALE

The Double PEC Wedge Problem: Diffraction and Total Far Field

Original
The Double PEC Wedge Problem: Diffraction and Total Far Field / Daniele, Vito; Lombardi, Guido; Zich, Rodolfo S.. - In: IEEE TRANSACTIONS ON ANTENNAS AND PROPAGATION. - ISSN 0018-926X. - STAMPA. - 66:12(2018), pp. 6482-6499. [10.1109/TAP.2018.2877260]

Availability:
This version is available at: 11583/2721545 since: 2018-12-21T16:58:16Z

Publisher:
IEEE-INST ELECTRICAL ELECTRONICS ENGINEERS INC

Published
DOI:10.1109/TAP.2018.2877260

Terms of use:

This article is made available under terms and conditions as specified in the corresponding bibliographic description in the repository

Publisher copyright
IEEE postprint/Author's Accepted Manuscript

©2018 IEEE. Personal use of this material is permitted. Permission from IEEE must be obtained for all other uses, in any current or future media, including reprinting/republishing this material for advertising or promotional purposes, creating new collecting works, for resale or lists, or reuse of any copyrighted component of this work in other works.

(Article begins on next page)

25 April 2024

The Double PEC Wedge Problem: Diffraction and Total Far Field

Vito Daniele, Guido Lombardi, *Senior Member, IEEE*, Rodolfo S. Zich, *Honorary Member, IEEE*

***Abstract*—Complex scattering targets are often made by structures constituted of wedges that may interact at near field. In this paper we examine the scattering of a plane electromagnetic wave by two separated arbitrarily oriented perfectly electrically conducting (PEC) wedges with parallel axes. The procedure to obtain the solution is based on the recently developed semi-analytical method known as Generalized Wiener-Hopf Technique (GWHT) that allows a comprehensive mathematical model of the problem in the spectral domain avoiding multiple steps of interaction among separated objects. The numerical results are presented to validate the procedure in terms of spectral quantities, GTD/UTD diffraction coefficients and total far fields for engineering applications. The structure is of interest in electromagnetic applications, in particular to accurately predict path-loss in propagation with diffraction phenomena.**

***Index Terms*—Wedges, Wiener-Hopf method, Integral equations, Electromagnetic diffraction, Near-field interactions, Propagation, Antenna technologies, Radar applications, EMC, Electromagnetic Shielding, Wireless communication.**

I. Introduction

THE accurate and efficient study of diffraction problems are of great interest in electromagnetic engineering communities, in particular when studying structures made of multiple wedges with near-field interactions. Moreover the quasi-analytical solution of canonical problems allow to investigate physical/engineering insights of the problem by decomposing the field into components. Moreover these solutions are useful to benchmark numerical codes.

In this paper we consider the classical canonical scattering problem constituted of two separated arbitrarily oriented Perfectly Electrically Conducting (PEC) wedges with parallel axes immersed in free-space with impedance Z_o and propagation constant k.

The problem is of interest for a variety of applications where field strength is a sensible topic. Examples of application comprehend propagation, radar technologies, antenna technologies, EMC, electromagnetic shielding, security scan in complex scenarios, wireless communication... In particular in electromagnetic propagation, fields diffracted by multiple objects are not exactly predicted by ray techniques. To improve the prediction of path loss in propagation with diffraction phenomena, we propose a new comprehensive model for the double PEC wedge problem that takes into account the entire structure in one shoot.

Manuscript received —; revised —.

The authors are with DET, Politecnico di Torino, Corso Duca degli Abruzzi 24, 10129 Torino, Italy, web: http://www.polito.it/ and with ISMB, Torino, Italy, web: http://www.ismb.it/ (emails: vito.daniele@polito.it, guido.lombardi@polito.it, rodolfo.zich@torinowireless.it).

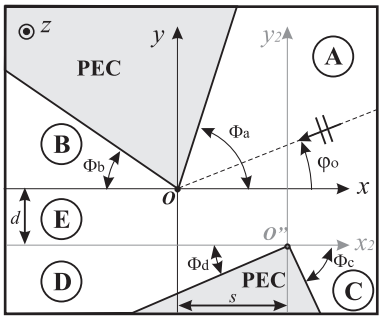

Fig. 1: Scattering of an electromagnetic wave by two PEC wedges. Two cartesian reference systems are reported, with coordinates (x, y, z) and (x_2, y_2, z) and centered respectively in O and O''. They are related together via $x_2 = x - s$, $y_2 = y + d$. Cylindrical coordinates (ρ, φ, z) centered in O and (ρ_2, φ_2, z) centered O'' are used too. The figure represents the case with positive s and d.

The proposed problem allows multiple configurations but for the sake of simplicity we make reference to Fig. 1 to illustrate the method. Cartesian coordinates as well as cylindrical coordinates are used to describe the problem. Two origins are considered: the edge of the upper wedge is chosen as origin O for coordinates (x, y, z) and (ρ, φ, z), while the edge of the lower wedge is chosen as origin O'' for coordinates (x_2, y_2, z) and (ρ_2, φ_2, z). The two reference systems are related together via $x_2 = x - s$, $y_2 = y + d$; corresponding cylindrical coordinate relations are easily derived. Fig. 1 shows the two PEC wedges respectively defined by $\rho > 0, \Phi_a < \varphi < \pi - \Phi_b$ and $\rho_2 > 0, -\pi + \Phi_d < \varphi_2 < -\Phi_c$ with translational symmetry along the z axis(parallel axes). To distinguish the same physical quantity defined with respect to different origins/coordinates we use the notation $\ddot{F}(x_2, y_2, z) = F(x, y, z) = \ddot{F}(\rho_2, \varphi_2, z) = F(\rho, \varphi, z)$. In the following we consider s as the staggered parameter along x and d as the distance along y between the x and x_2 axes(see Fig. 1). We assume d with positive values, while s can be either positive as in Fig. 1 or negative. Five regions are identified: region *A*, *B*, *C*, *D* are the angular regions delimited respectively by $0 < \varphi < \Phi_a$, $\pi - \Phi_b < \varphi < \pi$,$-\Phi_c < \varphi_2 < 0$, $-\pi < \varphi_2 < -\pi + \Phi_d$ (with $\Phi_f > 0$, $f = a, b, c, d$) and the layer region *E* with $-d < y < 0$.

In this work we consider time harmonic electromagnetic field with a time dependence specified by $e^{j\omega t}$ which is omitted. For the sake of simplicity, the structure is illuminated from region *A* by an E_z-polarized plane wave with azimuthal direction $\varphi = \varphi_o$ and with propagation constant k, however generalization to H_z polarization or skew incident case is possible and it doubles the equations.

$$E_z^i = E_o e^{jk\,\rho\cos(\varphi - \varphi_o)} \tag{1}$$

In diffraction theory the scattering by an isolated impenetrable wedge constitutes a fundamental wave problem with impact in different areas (electromagnetics, acoustics, fracture mechanics, elasticity...) and therefore it has been intensively studied. In particular several original methods had been conceived in the past [1]-[5] and they constitute a heritage of mathematical-physical literature. The most important spectral methods to study wedges are the Sommerfeld-Malyuzhinets (SM) technique (see [6]-[9] and reference therein) and the methods based on the Kontorovich-Lebedev (KL) transform (see [10]-[13] and reference therein).

Recently, the authors of this paper have proposed the Generalized Wiener-Hopf Technique (GWHT) that is a novel and effective spectral technique to solve electromagnetic problems constituted of isolated impenetrable and penetrable wedges (see [14]-[23] and reference therein).

The Wiener-Hopf (WH) method [24]-[26],[10],[23] is a well established technique to solve problems in all branches of engineering, mathematical physics and applied mathematics; a brief historical perspective is reported in [27]. In the last four decades, extensions of the technique by other authors have been reported, see for instance a non exhaustive bibliography [28]-[52],[27],[23] and references therein. In the authors' opinion, the GWHT together with the SM technique and the methods based on the KL transform completes the spectral techniques capable to handle isolated wedge problems.

Recently, the GWHT is able to further extend the class of solvable problems, in particular for the capability to handle complex scattering problems constituted of angular and rectangular/layer shapes (see [53]-[57] and references therein).

The GWHT can now easily formulate complex scattering problems in terms of Generalized Wiener-Hopf equations (GWHEs). Although, in general, the relevant GWHEs of the problems cannot be solved in closed form, this limit has been successfully overcome by resorting to the *Fredholm Factorization* [22]-[23]. The Fredholm factorization is a semi-analytical method that provides very accurate approximate solutions of GWHEs of a given problem. Its efficiency is based on the reduction of the classical factorization problem to system of Fredholm integral equations of second kind, by eliminating some of the WH unknowns via contour integration.

The application of the GWHT consists of four steps:

1) Deduction of GWHEs in spectral domain possibly with the help of equivalent network modelling,
2) Approximate solution via Fredholm factorization,
3) Analytic continuation of the approximate solution,
4) Evaluation of field with physical interpretation.

Taking inspiration from [58]-[59], in steps 1-2 network modelling orders and systematizes the procedure to obtain the spectral equations for complex problems avoiding redundancy, see for example [55] and reference therein. Moreover, in practice, steps 2 and 3 substitute the fundamental procedure of the classical WH technique [22]-[23], i.e. 1) the factorization of the kernel, 2) the computation of solution via decomposition and 3) the application of Liouville's Theorem.

In this paper the formulation of the double PEC wedge problem is done by applying the GWHT. Efficient approximate solutions are obtained via Fredholm factorization. Preliminary works on this topic has been presented in [60]-[63].

The literature shows several works that are related to the canonical problem examined in the paper; however, we assert that our method has the advantage to model the global structure with a true comprehensive mathematical model in spectral domain that avoids multiple steps of interaction among separated objects like in iterative physical optics or like in ray-tracing with multiple diffraction coefficients. Moreover the method is independent from the distance between the two wedges. Basically the solutions of the method are spectral quantities (WH unknowns) that contain the global information of fields. The benefit of the semi-analytical solution is that the solution can be analyzed in terms of field components via inverse spectral transformation and asymptotics (see for instance [56]-[57]). Moreover the mathematical model is valid for any $d > 0$ and s and therefore it allows the analysis of general configurations either with narrow wedges or with far wedges.

Focusing the attention on separated wedges, the literature presents related problems constituted of right angled wedges, apertures between two wedges, radiation from flanged waveguides and it ends with the current problem with non-coplanar wedges, see [64]-[81] and reference therein.

The paper is divided into eight Sections including the introduction. Section 2 presents the mathematical definitions and background preparatory to the WH equations of the five regions reported in Section 3. Section 4 shows the reduction of the equations to integral representations via Fredholm factorization. Both WH equations and the integral representations derived during the procedure can be easily interpreted as network relations. In the same Section the integral representations allow to obtain the factorization of the problem and the solution in terms of spectra. In particular Fredholm integral equations of second kind are derived for selected spectral unknowns. Section 5 is devoted to the analytic continuation of the approximate solution that is necessary to estimate physical/engineering quantities reported in Section 6 as GTD/UTD diffraction coefficients and total far fields. Finally Section 7 provides validation and convergence of the proposed method and it compares our results with the ones obtained by a fully numerical technique embedding singular modelling [82]-[84], thus demonstrating the superiority of the proposed semi-analytical technique for infinite canonical problems with respect to the case of finite structure. Conclusions are reported in Section 8.

II. Mathematical Definitions and Background

With reference to Fig. 1, considering the geometry and the source (1) of the problem, the field is independent from z and it has non-null $E_z(x,y), H_x(x,y), H_y(x,y)$ (from here on z dependence is omitted) that are governed by the wave equation. To meet mathematical requirements of WH technique small vanishing losses are assumed in the medium: $k = k' - jk''$ where $k', k'' > 0$ and $k'' << k'$. The starting point to deduce the Wiener-Hopf equations of the problem is to subdivide the entire geometry into the four angular regions (A,B,C,D) and the planar region (E) as described

in Section I. According to the coordinate systems and the notation described in Section I, the boundary conditions of the problem are: 1) zero E_z on the PEC faces, i.e. $E_z(\rho,\Phi_a)=E_z(\rho,\pi-\Phi_b)=0$ for any ρ, $\ddot{E}_z(\rho_2,-\Phi_c)=\ddot{E}_z(\rho_2,-\pi+\Phi_d)=0$ for any ρ_2; 2) continuity of E_z, H_x at interfaces $y=0,-d$, i.e. $E_z(x,0_-)=E_z(x,0_+)$, $H_x(x,0_-)=H_x(x,0_+)$, $E_z(x,-d_-)=E_z(x,-d_+), H_x(x,-d_-)=H_x(x,-d_+)$, with $y=0_\pm=\pm\delta$ and $y=-d_\pm=-d\pm\delta$ and vanishing $\delta>0$.

The formulation of the problem in the spectral domain is based on the definition of the Laplace/Fourier transforms:

$$\begin{cases} V_+^{up}(\sigma,\varphi)=\int_0^\infty E_z(\rho,\varphi)e^{j\sigma\rho}d\rho \\ I_+^{up}(\sigma,\varphi)=\int_0^\infty H_\rho(\rho,\varphi)e^{j\sigma\rho}d\rho \end{cases}, \quad (y\geq 0) \tag{2}$$

$$\begin{cases} v(\eta,y)=\int_{-\infty}^\infty E_z(x,y)e^{j\eta x}dx \\ i(\eta,y)=\int_{-\infty}^\infty H_x(x,y)e^{j\eta x}dx \end{cases}, \quad (-d\leq y\leq 0) \tag{3}$$

$$\begin{cases} V_+^{lw}(\sigma,\varphi_2)=\int_0^\infty \ddot{E}_z(\rho_2,\varphi_2)e^{j\sigma\rho_2}d\rho_2 \\ I_+^{lw}(\sigma,\varphi_2)=\int_0^\infty \ddot{H}_\rho(\rho_2,\varphi_2)e^{j\sigma\rho_2}d\rho_2 \end{cases}, \quad (y\leq -d) \tag{4}$$

The GWHEs are written in terms of the following quantities labeled axial spectral unknowns defined at $y=0$ (5) and $y_2=0$ (6):

$$\begin{array}{l} V_{1+}(\eta)=V_+^{up}(\sigma=\eta,0),\ I_{1+}(\eta)=I_+^{up}(\sigma=\eta,0), \\ V_{1\pi+}(\eta)=V_+^{up}(\sigma=\eta,-\pi),\ I_{1\pi+}(\eta)=I_+^{up}(\sigma=\eta,-\pi), \\ V_{1-}(\eta)=V_{1\pi+}(-\eta),\ I_{1-}(\eta)=-I_{1\pi+}(-\eta) \end{array} \tag{5}$$

$$\begin{array}{l} V_{2+}(\eta)=V_+^{lw}(\sigma=\eta,0),\ I_{2+}(\eta)=I_+^{lw}(\sigma=\eta,0), \\ V_{2\pi+}(\eta)=V_+^{lw}(\sigma=\eta,-\pi),\ I_{2\pi+}(\eta)=I_+^{lw}(\sigma=\eta,-\pi), \\ V_{2-}(\eta)=V_{2\pi+}(-\eta),\ I_{2-}(\eta)=-I_{2\pi+}(-\eta) \end{array} \tag{6}$$

In order to relate the axial spectral unknowns, located at the interface of the regions, we report the explicit definitions using cartesian coordinates:

$$\begin{cases} V_{1+}(\eta)=\int_0^\infty E_z(x,0)e^{j\eta x}dx;\ I_{1+}(\eta)=\int_0^\infty H_x(x,0)e^{j\eta x}dx, \\ V_{1\pi+}(\eta)=\int_{-\infty}^0 E_z(x,0)e^{-j\eta x}dx;\ I_{1\pi+}(\eta)=-\int_{-\infty}^0 H_x(x,0)e^{-j\eta x}dx \end{cases} \tag{7}$$

$$\begin{cases} V_{2+}(\eta)=\int_0^\infty \ddot{E}_z(x_2,0)e^{j\eta x_2}dx_2=e^{-j\eta s}\int_s^\infty E_z(x,-d)e^{j\eta x}dx, \\ I_{2+}(\eta)=\int_0^\infty \ddot{H}_x(x_2,0)e^{j\eta x_2}dx_2=e^{-j\eta s}\int_s^\infty H_x(x,-d)e^{j\eta x}dx, \\ V_{2\pi+}(\eta)=\int_{-\infty}^0 \ddot{E}_z(x_2,0)e^{-j\eta x_2}dx_2=e^{j\eta s}\int_{-\infty}^s E_z(x,-d)e^{-j\eta x}dx, \\ I_{2\pi+}(\eta)=-\int_{-\infty}^0 \ddot{H}_x(x_2,0)e^{-j\eta x_2}dx_2=-e^{j\eta s}\int_{-\infty}^s H_x(x,-d)e^{-j\eta x}dx \end{cases} \tag{8}$$

Furthermore, to obtain the GWHEs of the regions, we need to define the radial Laplace transform of the magnetic field along the PEC faces of the wedges:

$$I_{f+}(-m_f)=\int_0^\infty H_\rho(\rho,\varphi_f)e^{-jm_f\rho}d\rho=I_+^{up}(\sigma=-m_f,\varphi_f),\ f=a,b \tag{9}$$

with $\varphi_a=\Phi_a$, $\varphi_b=\pi-\Phi_b$; and

$$I_{f+}(-m_f)=\int_0^\infty \ddot{H}_{\rho_2}(\rho_2,\varphi_{2f})e^{-jm_f\rho_2}d\rho_2=I_+^{lw}(\sigma=-m_f,\varphi_{2f}),\ f=c,d \tag{10}$$

with $\varphi_{2c}=-\Phi_c$, $\varphi_{2d}=-\pi+\Phi_d$.

With reference, for instance, to the η complex plane, the spectral unknowns are labeled with $\pm$ subscripts: $+$ indicates plus functions in the complex plane η, *i.e.* functions that converge in an upper half-plane ($Im[\eta]>Im[\eta_{up}]$); conversely $-$ indicates minus functions that converge in a lower half-plane ($Im[\eta]<Im[\eta_{lo}]$). The $+$ ($-$) functions are considered non-conventional (non-standard) if $Im[\eta_{up}]>0$ ($Im[\eta_{lo}]<0$). We recall that we have selected propagation constant k with a negative (vanishing) imaginary part to mostly avoid the presence of singularities on the real axis of the η plane.

According to our problem the Laplace transform of the source E_z^i (1) at $y=0$ is

$$V_{1+}^i(\eta)=\int_0^\infty E_z^i(x,0)e^{j\eta x}dx=\frac{jE_o}{\eta-\eta_o} \tag{11}$$

with a pole $\eta_o=-k\cos(\varphi_o)$ whose location in η complex plane depends on the incident angle φ_o (i.e. η_o is in the 2nd or 4th quadrant along the segment that connects k to $-k$).

From (3) and (7)-(8) we note that

$$\begin{cases} v(\eta,y=0)=V_{1+}(\eta)+V_{1\pi+}(-\eta) \\ i(\eta,y=0)=I_{1+}(\eta)-I_{1\pi+}(-\eta) \end{cases} \tag{12}$$

$$\begin{cases} v(\eta,y=-d)=e^{j\eta s}V_{2+}(\eta)+e^{j\eta s}V_{2\pi+}(-\eta) \\ i(\eta,y=-d)=e^{j\eta s}I_{2+}(\eta)-e^{j\eta s}I_{2\pi+}(-\eta) \end{cases} \tag{13}$$

In the following Sections we examine each region starting from the GWHEs to obtain the relevant integral representations by contour integration. In particular we use the contours $\gamma_{1\eta}$ and $\gamma_{2\eta}$ that are respectively the *smile* and the *frown* integration line in η-plane [22]-[23], i.e. the real axis of η'-plane indented at $\eta'=\eta$ with a small semi-circumference respectively in the lower and in the upper half plane.

The application of Fredholm factorization is based on integral decomposition of the Wiener-Hopf unknowns. The classical decomposition equations (see Ch. 3 of [23]) apply to conventional (or standard) plus functions. Non-standard functions, due to the presence of poles located in the standard conventional regular half-plane, require modified Cauchy decompositions formula:

$$\begin{array}{ll} \frac{1}{2\pi j}\int_{\gamma_{1\eta}}\frac{F_+(\eta')}{\eta'-\eta}d\eta'=F_+(\eta)-F_+^{ns}(\eta), & \frac{1}{2\pi j}\int_{\gamma_{2\eta}}\frac{F_+(\eta')}{\eta'-\eta}d\eta'=-F_+^{ns}(\eta) \\ \frac{1}{2\pi j}\int_{\gamma_{2\eta}}\frac{F_-(\eta')}{\eta'-\eta}d\eta'=-F_-(\eta)+F_-^{ns}(\eta), & \frac{1}{2\pi j}\int_{\gamma_{1\eta}}\frac{F_-(\eta')}{\eta'-\eta}d\eta'=F_-^{ns}(\eta) \end{array} \tag{14}$$

for $\eta\in\mathbb{R}$ and where $F_+^{ns}(\eta)$ and $F_-^{ns}(\eta)$ are the non-standard part of $F_+(\eta)$ and $F_-(\eta)$. To demonstrate this result, we recall that $\int_{\Gamma_{1\eta}}\frac{F_+(\eta')}{\eta'-\eta}d\eta'\to 0$ ($\int_{\Gamma_{2\eta}}\frac{F_-(\eta')}{\eta'-\eta}d\eta'\to 0$) where $\Gamma_{1\eta}$ ($\Gamma_{2\eta}$) is the half-circumference with radius $|\eta|\to\infty$ in the upper(lower) η half-plane. Note that (14) hold for $\eta\in\mathbb{R}$. From here on, this assumption is valid unless otherwise specified.

We assert that, in scattering problems with plane wave excitation, the non-standard parts derive from Geometrical Optics (GO) contributions and they are known a priori using ray theory. Finally, in this paper we denote the azimuthal direction of GO waves with φ_{lab} where the subscripts lab are in upper case (lower case) if referred to a wave that leaves (approaches)

the wedges: for instance, the wave reflected from the PEC face at $\varphi = \Phi_a$ propagates as $e^{jk_o\rho\cos(\varphi-\varphi_{ra})} = e^{-jk_o\rho\cos(\varphi-\varphi_{RA})}$ with $\varphi_{ra} = 2\Phi_a - \varphi_o$ and $\varphi_{RA} = \varphi_{ra} - \pi$ with respect to the reference O of Fig. 1. In the following we use the dummy pedex go to refer to quantities related to an incoming GO wave with direction φ_{go}.

III. GWHEs of the Problem

Starting from the definitions reported in the previous Sections we define the GWHEs for each of the five regions of the problem at E_z polarization.

A. Angular regions

According to the theory presented in [14]-[15] and using the definitions of axial spectral unknowns (5)-(6) and radial Laplace transforms of field components at PEC faces (9)-(10), the GWHEs of the angular regions A,B,C,D are respectively

$$\begin{cases} Y_c(\eta)\, V_{1+}(\eta) - I_{1+}(\eta) = -I_{a+}(-m_a(\eta)) \\ Y_c(\eta)\, V_{1\pi+}(\eta) + I_{1\pi+}(\eta) = I_{b+}(-m_b(\eta)) \\ Y_c(\eta)\, V_{2+}(\eta) + I_{2+}(\eta) = I_{c+}(-m_c(\eta)) \\ Y_c(\eta)\, V_{2\pi+}(\eta) - I_{2\pi+}(\eta) = -I_{d+}(-m_d(\eta)) \end{cases} \tag{15}$$

where $Y_c(\eta) = \frac{1}{Z_c(\eta)} = \frac{\xi(\eta)}{kZ_o}$ is the free-space spectral admittance defined in terms of the free space impedance $Z_o = 1/Y_o$ and the free-space spectral propagation constant $\xi(\eta) = \sqrt{k^2 - \eta^2}$ with the assumption of the proper sheet of η plane to be such that $\xi(\eta = 0) = k$.

Note that the spectral unknowns $I_{f+}(-m_f(\eta))$ ($f = a, b, c, d$) defined on the faces of the wedges depend on the spectral variables m_f related to the η complex plane via

$$m_f(\eta) = -\eta\cos\Phi_f + \xi(\eta)\sin\Phi_f \tag{16}$$

Equations (15) are GWHEs since the plus-η and minus-$m_f(\eta)$ unknowns are defined into different complex planes although related together. An important result is that a suitable mapping depending on the aperture angle Φ_f of the angular region reduces each of them to a classical WH equation in a new complex plane $\overline{\eta}_f$, $f = a, b, c, d$ [14]-[15]:

$$\overline{\eta}_f = -k\cos\left(\frac{\pi}{\Phi_f}\arccos\left(-\frac{\eta}{k}\right)\right),\ f = a, b, c, d \tag{17}$$

B. Layered region

According to the classical spectral theory of layered regions based on transmission line modeling [23],[58], the following two-port model holds for region E in terms of the Fourier transforms of field components (3) defined at $y = 0, -d$:

$$\begin{cases} -i(\eta, 0) = Y_{11}(\eta)v(\eta, 0) + Y_{12}(\eta)v(\eta, -d) \\ i(\eta, -d) = Y_{21}(\eta)v(\eta, 0) + Y_{22}(\eta)v(\eta, -d) \end{cases} \tag{18}$$

where

$$\begin{aligned} Y_{11}(\eta) = Y_{22}(\eta) &= -jY_c(\eta)\cot[\xi(\eta)d] \\ Y_{12}(\eta) = Y_{21}(\eta) &= j\frac{Y_c(\eta)}{\sin[\xi(\eta)d]} \end{aligned} \tag{19}$$

By using (12) and (13) we obtain (20) in terms of axial spectral unknowns. Note that the $\pi+$ functions in $-\eta$ are minus unknowns in η (6) and by changing η with $-\eta$ in (20) we obtain two additional GWHEs that are useful to make symmetrical the system of equations even if we introduce extra unknowns related to the original ones (note that $Y_{ij}(-\eta) = Y_{ij}(\eta)$, $i, j = 1, 2$ since they depend on η through $\xi(\eta)$).

IV. Fredholm factorization of the Problem

The reduction of the GWHEs (15), (20) and modified (20) ($\eta \to -\eta$) to integral representations that allows to obtain a system of Fredholm integral equations (FIEs) of second kind for the solution of the problem constitutes the central point of the proposed procedure. While the classical factorization separates the minus unknowns from the plus unknowns by manipulating the whole WH system of equations, the Fredholm factorization simply eliminates time after time some of the unknowns by contour integration (14). The main advantage of Fredholm factorization is that it is always applicable. Furthermore the procedure is independent from the geometrical form of the space located out of the considered region. One of the main advantages is that the integral representations can be obtained once and for all, by studying time after time one single region. These characteristics of the Fredholm factorization notably simplify the deduction of the FIEs of the whole problem. In particular, network representations for integral representations of WH equations [23],[55]-[57],[60] turn out to be very useful since they model the whole problem as an electrical network having as components the multiports representing the single region. We anticipate that in the final Fredholm equations the non-standard parts of the spectra derived from (14) constitute the known second members of the FIEs. If we eliminate minus functions, the Fredholm factorization yields integral representations that couples the plus functions. From here until the final FIEs, the observation point is assumed always real in the spectral plane η. We note that the formulation of our problem contains exponential behaviour $e^{\pm j\eta s}$ (20), however the application of (14) is valid since the closures of integration lines with half- circumferences at infinity still give vanishing contributions [60].

In the following we focus the attention on one of the angular regions, region A, and then we extrapolate the integral representations of the angular regions B,C,D from it. Second, we obtain the integral representation of the finite layer region E. All integral representations are then interrelated as network models and from them we derive the system of FIEs to get the spectral solution of the problem.

A. Integral representation for the angular regions

With reference to region A ($0 \le \varphi < \Phi_a$), ($y > 0$) at E_z polarization the GWHE of this region is the first equation reported in (15). By applying to the equation the mapping (17) specified for this region ($\bar{\eta}_a(\eta) = \alpha(\eta)$)

$$\begin{aligned} \eta(\alpha) &= -k\cos\left[\tfrac{\Phi_a}{\pi}\arccos(-\tfrac{\alpha}{k})\right] \\ \alpha(\eta) &= -k\cos\left[\tfrac{\pi}{\Phi_a}\arccos(-\tfrac{\eta}{k})\right] \end{aligned} \tag{21}$$

we obtain the following Classical Wiener-Hopf Equation (CWHE) [14]-[15] in α plane

$$\bar{Y}_c(\alpha)\,\bar{V}_{1+}(\alpha) - \bar{I}_{1+}(\alpha) = -\bar{I}_{a+}(-\alpha) \tag{22}$$

where

$$V_{1+}(\eta) = \bar{V}_{1+}(\alpha),\ I_{1+}(\eta) = \bar{I}_{1+}(\alpha),\ I_{a+}(-m_a) = \bar{I}_{a+}(-\alpha) \tag{23}$$

and $Y_c(\eta) = \bar{Y}_c(\alpha)$. $\bar{V}_{1+}(\alpha)$ and $\bar{I}_{1+}(\alpha)$ are plus functions in α plane while $\bar{I}_{a+}(-\alpha)$ is a minus function in α [14]. Note

$$\begin{cases} -I_{1+}(\eta)+I_{1\pi+}(-\eta)=Y_{11}(\eta)[V_{1+}(\eta)+V_{1\pi+}(-\eta)]+Y_{12}(\eta)[V_{2+}(\eta)+V_{2\pi+}(-\eta)]e^{j\eta s} \\ e^{j\eta s}(I_{2+}(\eta)-I_{2\pi+}(-\eta))=Y_{21}(\eta)[V_{1+}(\eta)+V_{1\pi+}(-\eta)]+Y_{22}(\eta)[V_{2+}(\eta)+V_{2\pi+}(-\eta)]e^{j\eta s} \end{cases} \quad (20)$$

that in general plus functions in η and minus functions in m_a are respectively plus functions in α and minus functions in α but the viceversa is not true.

To obtain the integral representation of the angular region, we apply the contour integration with the help of (14) in α plane that allows to eliminate one of the unknowns. In order to eliminate $\bar{I}_{a+}(-\alpha)$, we apply the contour integration to (22) along the contour $\gamma_{1\alpha}$ which is the smile integration line:

$$\frac{1}{2\pi j}\int_{\gamma_{1\alpha}}\frac{\bar{Y}_c(\alpha')\,\bar{V}_{1+}(\alpha')-\bar{I}_{1+}(\alpha')}{\alpha'-\alpha}d\alpha'=-\frac{1}{2\pi j}\int_{\gamma_{1\alpha}}\frac{\bar{I}_{a+}(-\alpha')}{\alpha'-\alpha}d\alpha' \quad (24)$$

To proceed with the estimation of (24) we need to examine the spectral content of the quantities/unknowns reported in the equation. The use of (14) yields attention on non-standard poles of the spectral unknowns whose origin is related to the considered source excitation, in our case an E_z plane wave (1). Since the source is constituted of a plane wave, only Geometrical Optics (GO) components with infinite support gives poles in the spectra of the unknowns, i.e. incident plane wave, reflected plane waves, multiple reflected plane waves. The infinite support of the GO components is a mathematical requirement (Laplace transform) to get poles in the spectrum. Moreover the delay-phase shift of the GO components in (24) due to the staggered parameter s (that generates shadow boundaries) does not yield any contribution on the residue of the Laplace transform of the GO components since they are defined less than a field component with finite support (the shadow) that is an entire function in Laplace domain.

First, let us focus on the incident plane wave with incoming direction φ_o, outgoing direction $\varphi_I=\pi-\varphi_o$. From (11) we note that the incident wave induces the pole $\eta_o=-k\cos\varphi_o$ in the η plane and taking into account (21) the spectral quantities in α plane show the pole $\alpha_o=\alpha(\eta_o)=-k\cos\frac{\pi}{\Phi_a}\varphi_o$. As the incident wave each GO component with infinite support of the field induces a pole $\eta_{go}=-k\cos\varphi_{go}$ and $\alpha_{go}=\alpha(\eta_{go})=-k\cos\frac{\pi}{\Phi_a}\varphi_{go}$ according to the incoming direction of propagation φ_{go}. The location of poles in the spectral planes η and α (upper or lower half planes) is directly related to the incoming direction φ_{go}. From the studies of GO poles we define the standard properties of plus and minus unknowns in the GWHEs and in particular here in (24).

Since $\bar{I}_{a+}(-\alpha)$ is a minus function in the α-plane, closing at infinity the smile integration line $\gamma_{1\alpha}$ in the lower half α-plane, we capture the GO poles α_{go} with $\Phi_a/2<\varphi_{go}<\Phi_a$ (Residue theorem). From (14) in α plane, the RHS (Right-Hand-Side) of (24) is equal to

$$-\frac{1}{2\pi j}\int_{\gamma_{1\alpha}}\frac{\bar{I}_{a+}(-\alpha')}{\alpha'-\alpha}d\alpha'=-\sum_{\alpha_{go}}\frac{R_{ia\alpha}}{\alpha-\alpha_{go}}u(\varphi_{go}-\frac{\Phi_a}{2}) \quad (25)$$

where $u(\cdot)$ is the unitstep function (Heaviside) and $R_{ia\alpha}$ are the residues of $\bar{I}_{a+}(-\alpha)$ at α_{go} that can be computed directly in $m_a(\eta)$ plane using

$$R_{ia\alpha}=R_{iam}\left.\frac{d\alpha}{dm_a}\right|_{m_{ago}} \quad (26)$$

and R_{iam} are the residues of the Laplace transform $I^{GO}_{a+}(-m_a)$ of the primary GO field $H^{GO}_{\rho}(\rho,\Phi_a)$ at $m_{ago}=k\cos(\Phi_a-\varphi_{go})$.

Focusing the attention on the second contribution of the LHS (Left-Hand-Side) of (24) and closing at infinity the smile integration line $\gamma_{1\alpha}$ in the upper half α-plane, we obtain through Residue theorem and using (14)

$$\frac{1}{2\pi j}\int_{\gamma_{1\alpha}}\frac{\bar{I}_{1+}(\alpha')}{\alpha'-\alpha}d\alpha'=\bar{I}_{1+}(\alpha)-\sum_{\alpha_{go}}\frac{R_{i\alpha}}{\alpha-\alpha_{go}}u(-\varphi_{go}+\frac{\Phi_a}{2}) \quad (27)$$

where $R_{i1\alpha}$ are the residues of $\bar{I}_{1+}(\alpha)$ at α_{go}

$$R_{i1\alpha}=R_{i1\eta}\left.\frac{d\alpha}{d\eta}\right|_{\eta_{go}} \quad (28)$$

and $R_{i1\eta}$ are the residues of the Laplace transform $I^{GO}_{1+}(\eta)$ of the primary GO field $H^{GO}_{\rho}(\rho,0)$ at $\eta_{go}=-k\cos(\varphi_{go})$.

Taking into account (24), we complete the integral representation in η plane by considering the first term of the LHS:

$$\begin{aligned}\tfrac{1}{2\pi j}\int_{\gamma_{1\alpha}}\tfrac{\bar{Y}_c(\alpha')\,\bar{V}_{1+}(\alpha')}{\alpha'-\alpha}d\alpha'&=\tfrac{1}{2\pi j}\int_{\bar{\gamma}_{1\alpha}}\tfrac{\bar{Y}_c(\alpha(\eta'))\,\bar{V}_{1+}(\alpha(\eta'))}{\alpha(\eta')-\alpha(\eta)}\tfrac{d\alpha}{d\eta'}d\eta'= \\ &=\tfrac{1}{2\pi j}\int_{\bar{\gamma}_{1\alpha}}\tfrac{Y_c(\eta')\,V_{1+}(\eta')}{\alpha(\eta')-\alpha(\eta)}\tfrac{d\alpha}{d\eta'}d\eta'\end{aligned} \quad (29)$$

where $\bar{\gamma}_{1\alpha}$ is the image in η plane of the smile integration line $\gamma_{1\alpha}$ defined in α plane and where the inverse mapping $\alpha=\alpha(\eta)$ of (21) is used. The next step is to warp in η plane the contour $\bar{\gamma}_{1\alpha}$ into $\gamma_{1\eta}$. The warping can capture singularities either of the integral kernel $1/(\alpha(\eta')-\alpha(\eta))$ or of the unknowns as GO poles located in the proper sheet of η plane (see definition in Section III-A). Let us discuss later the singularities of the integral kernel and by taking into account the GO singularities we have

$$\begin{aligned}&\tfrac{1}{2\pi j}\int_{\bar{\gamma}_{1\alpha}}\tfrac{Y_c(\eta')\,V_{1+}(\eta')}{\alpha(\eta')-\alpha(\eta)}\tfrac{d\alpha}{d\eta'}d\eta'=\tfrac{1}{2\pi j}\int_{\gamma_{1\eta}}\tfrac{Y_c(\eta')\,V_{1+}(\eta')}{\alpha(\eta')-\alpha(\eta)}\tfrac{d\alpha}{d\eta'}d\eta'+ \\ &-\textstyle\sum_{\alpha_{go}}\tfrac{Y_c(\eta_{go})R_{v1\alpha}}{\alpha(\eta)-\alpha_{go}}(u(\tfrac{\Phi_a}{2}-\varphi_{go})-u(\tfrac{\pi}{2}-\varphi_{go}))\end{aligned} \quad (30)$$

where $R_{v1\alpha}$ are the residues of $\bar{V}_{1+}(\alpha)$ at α_{go}

$$R_{v1\alpha}=R_{v1\eta}\left.\frac{d\alpha}{d\eta}\right|_{\eta_{go}} \quad (31)$$

with $R_{v1\eta}$ residues at $\eta_{go}=-k\cos(\varphi_{go})$ of $V^{GO}_{1+}(\eta)$ which is the Laplace transform of the primary GO field $E^{GO}_z(\rho,0)$.

Since our aim is to obtain an integral representation in η plane, using (25), (27) and (30), (24) becomes

$$\begin{aligned}&\tfrac{1}{2\pi j}\textstyle\int_{\gamma_{1\eta}}\tfrac{Y_c(\eta')\,V_{1+}(\eta')}{\alpha(\eta')-\alpha(\eta)}\tfrac{d\alpha}{d\eta'}d\eta'=I_{1+}(\eta)-\sum_{\alpha_{go}}\tfrac{R_{ia\alpha}u(\varphi_{go}-\frac{\Phi_a}{2})}{\alpha(\eta)-\alpha_{go}}+ \\ &-\textstyle\sum_{\alpha_{go}}\tfrac{R_{i1\alpha}u(-\varphi_{go}+\frac{\Phi_a}{2})}{\alpha(\eta)-\alpha_{go}}-\sum_{\alpha_{go}}\tfrac{Y_c(\eta_{go})R_{v1\alpha}(u(\frac{\pi}{2}-\varphi_{go})-u(\frac{\Phi_a}{2}-\varphi_{go}))}{\alpha(\eta)-\alpha_{go}}\end{aligned} \quad (32)$$

We note that (32) is an integral representation that relates the spectral unknowns $V_{1+}(\eta)$ and $I_{1+}(\eta)$. However this representation is with singular kernel. The next step consists of deriving a new integral representation with compact kernel by means of regularization. We observe that integrating $V_{1+}(\eta)$ along the contour $\gamma_{2\eta}$ and closing the contour at infinity in the upper half η-plane, from (14) we obtain

$$\frac{1}{2\pi j}\int_{\gamma_{2\eta}}\frac{Y_c(\eta)\,V_{1+}(\eta')}{\eta'-\eta}d\eta' = -\sum_{\eta_{go}}\frac{Y_c(\eta)R_{v1\eta}}{\eta-\eta_{go}}u(\frac{\pi}{2}-\varphi_{go}) \quad (33)$$

Subtracting (33) from (32) it yields

$$Y_c(\eta)V_{1+}(\eta)-I_{1+}(\eta)+\frac{1}{2\pi j}\int_{-\infty}^{\infty}\left(\frac{Y_c(\eta')\frac{d\alpha}{d\eta'}}{\alpha(\eta')-\alpha(\eta)}-\frac{Y_c(\eta)}{\eta'-\eta}\right)V_{1+}(\eta')d\eta' = I_{ca}(\eta) \quad (34)$$

where $I_{ca}(\eta)$ is the source of the integral representation (34) that is the combination of all sums appearing in (32) and (33).

Note that $I_{ca}(\eta)$ depends on the GO field of the complete problem (easily obtainable by GO analysis ignoring delay-phase shift), while the kernel of (34) depends only on the geometrical parameters of region A.

Going back to the kernel singularities as outlined before (30), we need to investigate their effect in (34) to get a general integral representation that is valid on the real axis of the proper sheet of η plane. The regularization procedure has removed the singularity at $\eta'=\eta$ in (34), however the integrand can be singular for $\eta'\neq\eta$ due to the roots of $\alpha(\eta')-\alpha(\eta)$. The roots $\eta'=p_n^{\Phi_a}(\eta)=\eta\cos(2n\Phi_a)-\xi(\eta)\sin(2n\Phi_a)$, $n\in\mathbb{N}_0$ (see (94) for details) in the proper sheet define singularity lines that, if crossed by the observation point η, can give further contributions (correction terms) in the derivation of the integral representation (34). Therefore the accurate location of $p_n^{\Phi_a}(\eta)$ in relation to the amplitude of Φ_a is of great importance. If $p_n^{\Phi_a}(\eta)$ is located in the upper half proper η plane, the singularity gives contribution since it is captured while closing the integration contours to derive the integral representation. In this case we need to compute the value of $V_{1+}(p_n^{\Phi_a}(\eta))$ (due to the singularity lines) in terms of $V_{1+}(\eta)$ by using the Cauchy's integral formula, see eqs. (71) of [55]. Note that this expression of $V_{1+}(p_n^{\Phi_a}(\eta))$ is zero for $p_n^{\Phi_a}(\eta)$ located in the lower half proper η plane.

The final integral representation is reported in (35) for real η and η', however the same eq. is valid for integration line different from the real axis but with observation points lying on the integration line [55].

$$I_{1+}(\eta)=\mathcal{Y}_a[V_{1+}(\eta)]-I_{sca}(\eta) \quad (35)$$

with

$$\mathcal{Y}_a[...]=Y_c(\eta)+\frac{1}{2\pi j}\int_{-\infty}^{\infty}y_a(\eta,\eta')[...]d\eta \quad (36)$$

$$y_a(\eta,\eta')=\frac{Y_c(\eta')}{\alpha(\eta')-\alpha(\eta)}\frac{d\alpha}{d\eta'}-\frac{Y_c(\eta)}{\eta'-\eta}+\sum_{n=1}^{+\infty}\frac{q_n^{\Phi_a}(\eta)u(\frac{\pi}{2}-n\Phi_a)}{\eta'-\mathrm{p}_n^{\Phi_a}(\eta)} \quad (37)$$

$$p_n^{\Phi_a}(\eta) = \eta\cos 2n\Phi_a-\sqrt{k^2-\eta^2}\sin 2n\Phi_a \quad (38)$$

$$q_n^{\Phi_a}(\eta) = \frac{1}{kZ_o}(\eta\sin 2n\Phi_a+\sqrt{k^2-\eta^2}\cos 2n\Phi_a) \quad (39)$$

$$I_{sca}(\eta)=I_{ca}(\eta)-\sum_{n=1}^{+\infty}q_n^{\Phi_a}(\eta)V_{1+}^{ns}(\mathrm{p}_n^{\Phi_a}(\eta))u(\frac{\pi}{2}-n\Phi_a) \quad (40)$$

For obtuse aperture angle ($\pi/2<\Phi_a<\pi$) (35) reduces to (34) since no singularity line is captured. Eq. (35) is valid also for observation points η near the integration line till a new singularity line $\eta'=p_n^{\Phi_a}(\eta)$ is crossed. In this case, to get a representation with extended validity we need to consider further contribution due to the singularity. This behaviour is known in literature as sectional analytic function [85].

In (35) we have used an abstract notation that is associated to a network interpretation of the integral representation. In particular region A is modelled via a one port network (Norton model) where the current $I_{1+}(\eta)$ is related to the voltage $V_{1+}(\eta)$ through the algebraic-integral operator admittance $\mathcal{Y}_a[...]$ and the short circuit current $I_{sca}(\eta)$. Pictorial illustration of the model is given in Fig. 2.

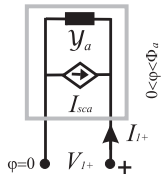

Fig. 2: Norton equivalent network model of region A corresponding to (35).

We can extrapolate (or rigorously demonstrate as per region A) that region B, C, and D have integral representations/network models similar to region A.

For region B, starting from 2nd eq. of (15), the final representation for real η and η' is:

$$I_{1\pi+}(\eta)=-\mathcal{Y}_b[V_{1\pi+}(\eta)] \quad (41)$$

with

$$\mathcal{Y}_b[...]=Y_c(\eta)+\frac{1}{2\pi j}\int_{-\infty}^{\infty}y_b(\eta,\eta')[...]d\eta \quad (42)$$

$$y_b(\eta,\eta')=\frac{Y_c(\eta')}{\beta(\eta')-\beta(\eta)}\frac{d\beta}{d\eta'}-\frac{Y_c(\eta)}{\eta'-\eta}+\sum_{n=1}^{+\infty}\frac{q_n^{\Phi_b}(\eta)u(\frac{\pi}{2}-n\Phi_b)}{\eta'-\mathrm{p}_n^{\Phi_b}(\eta)} \quad (43)$$

$$p_n^{\Phi_b}(\eta) = \eta\cos 2n\Phi_b-\sqrt{k^2-\eta^2}\sin 2n\Phi_b \quad (44)$$

$$q_n^{\Phi_b}(\eta) = \frac{1}{kZ_o}(\eta\sin 2n\Phi_b+\sqrt{k^2-\eta^2}\cos 2n\Phi_b) \quad (45)$$

$$\beta(\eta) = -k\cos\left[\frac{\pi}{\Phi_b}\arccos(-\frac{\eta}{k})\right] \quad (46)$$

Note in (41) the absence of a short circuit current (source of the integral representation). In fact, since we have assumed plane wave illumination from region A, the spectra of the unknowns in region B are free from pole singularities that arise only from GO components with infinite support (finite support GO component yields entire function in Laplace domain).

For region C, starting from 3rd eq. of (15), the final representation for real η and η' is:

$$I_{2+}(\eta)=-\mathcal{Y}_c[V_{2+}(\eta)]+I_{scc}(\eta) \quad (47)$$

with

$$\mathcal{Y}_c[...]=Y_c(\eta)+\frac{1}{2\pi j}\int_{-\infty}^{\infty}y_c(\eta,\eta')[...]d\eta \quad (48)$$

$$y_c(\eta,\eta')=\frac{Y_c(\eta')}{\gamma(\eta')-\gamma(\eta)}\frac{d\gamma}{d\eta'}-\frac{Y_c(\eta)}{\eta'-\eta}+\sum_{n=1}^{+\infty}\frac{q_n^{\Phi_c}(\eta)u(\frac{\pi}{2}-n\Phi_c)}{\eta'-\mathrm{p}_n^{\Phi_c}(\eta)} \quad (49)$$

$$p_n^{\Phi_c}(\eta) = \eta\cos 2n\Phi_c - \sqrt{k^2-\eta^2}\sin 2n\Phi_c \quad (50)$$

$$q_n^{\Phi_c}(\eta) = \frac{1}{kZ_o}(\eta\sin 2n\Phi_c + \sqrt{k^2-\eta^2}\cos 2n\Phi_c) \quad (51)$$

$$\gamma(\eta) = -k\cos\left[\frac{\pi}{\Phi_c}\arccos(-\frac{\eta}{k})\right] \quad (52)$$

$$I_{scc}(\eta) = I_{cc}(\eta) - \sum_{n=1}^{+\infty} q_n^{\Phi_c}(\eta)V_{2+}^{ns}(\mathrm{p}_n^{\Phi_c}(\eta))u(\frac{\pi}{2}-n\Phi_c) \quad (53)$$

Note that $I_{cc}(\eta)$ depends on the GO field of the complete problem as discussed for region A and it is related to the spectra of the unknowns of 3rd eq. in (15), i.e. the non-standard residue/poles of $V_{2+}(\eta)$, $I_{2+}(\eta)$, $I_{c+}(-m_c(\eta))$.

Finally, from the 4th eq. of (15), region D shows for real η and η' the model

$$I_{2\pi+}(\eta) = \mathcal{Y}_d[V_{2\pi+}(\eta)] \quad (54)$$

with

$$\mathcal{Y}_d[...] = Y_d(\eta) + \frac{1}{2\pi j}\int_{-\infty}^{\infty} y_d(\eta,\eta')[...]d\eta \quad (55)$$

$$y_d(\eta,\eta') = \frac{Y_c(\eta')}{\delta(\eta')-\delta(\eta)}\frac{d\delta}{d\eta'} - \frac{Y_c(\eta)}{\eta'-\eta} + \sum_{n=1}^{+\infty}\frac{q_n^{\Phi_d}(\eta)u(\frac{\pi}{2}-n\Phi_d)}{\eta'-\mathrm{p}_n^{\Phi_d}(\eta)} \quad (56)$$

$$p_n^{\Phi_d}(\eta) = \eta\cos 2n\Phi_d - \sqrt{k^2-\eta^2}\sin 2n\Phi_d \quad (57)$$

$$q_n^{\Phi_d}(\eta) = \frac{1}{kZ_o}(\eta\sin 2n\Phi_d + \sqrt{k^2-\eta^2}\cos 2n\Phi_d) \quad (58)$$

$$\delta(\eta) = -k\cos\left[\frac{\pi}{\Phi_d}\arccos(-\frac{\eta}{k})\right] \quad (59)$$

As per region B no source is present in the integral representation (54), for the absence of GO components with infinite support.

Eqs. (41),(47),(54) extend their validity for observation point η out of the integration line as commented for region A (model (35)).

As per region A, the three angular regions B,C,D show integral representations (respectively (41) (47), (54)) that can be interpreted as abstract network models. Pictorial illustrations of the models are given in Fig. 3.

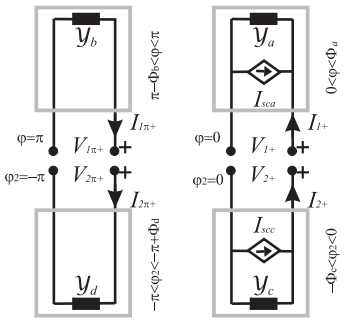

Fig. 3: Norton equivalent network model of regions B, A, C, D in the same geometrical order as reported in Fig. 1 and corresponding respectively to (41),(35),(47),(54).

B. Integral representation for the layer region

With reference to region E ($-d < y < 0$) at E_z polarization the GWHEs of this region are given in (20). Note that in this case the unknowns are defined in the same complex plane η as in classical WH equations but a problematic exponential behavior depending on the staggered parameter s is present. Interesting attempts to deal with exponential factors in WH equations based on weak factorization are reported in [33],[34],[52] and references therein.

In this paper we propose a novel effective method to deal with exponential factors in WH equations that is based on Fredholm factorization [22]-[23], [86].

Based on the observation made at the end of Section III-B, we double the equations reported in (20) by interchanging η with $-\eta$. Using the Fredholm factorization we eliminate the minus functions respectively $I_{1\pi+}(-\eta)$, $I_{2\pi+}(-\eta)$ in the original version of (20) and $I_{1+}(-\eta)$, $I_{2+}(-\eta)$ in the modified (20) while interchanging η with $-\eta$. The result is integral representations that relates the plus unknowns, i.e the plus currents $[I_{1+}(\eta), I_{2+}(\eta), I_{1\pi+}(\eta), I_{2\pi+}(\eta)]$ to the plus voltages $[V_{1+}(\eta), V_{2+}(\eta), V_{1\pi+}(\eta), V_{2\pi+}(\eta)]$.

Let us focus the procedure on the original 1st eq of (20) and then we extrapolate the integral representations of the other three equations. To obtain the relevant integral representation, we apply the contour integration $\gamma_{1\eta}$ with the help of (14) that allows to eliminate the unknown $I_{1\pi+}(-\eta)$ which is a standard minus unknown in η ($I_{1\pi+}^{ns}(-\eta) = 0$ since no GO component with infinite support is present). The left-hand side (LHS) of the 1st eq in (20) yields

$$\frac{1}{2\pi j}\int_{\gamma_{1\eta}}\frac{-I_{1+}(\eta')+I_{1\pi+}(-\eta')}{\eta'-\eta}d\eta' = -I_{1+}(\eta) + I_{1+}^{ns}(\eta) \quad (60)$$

Repeating the $\gamma_{1\eta}$ integration on the right-hand side (RHS) of the 1st eq. in (20), it yields

$$\frac{1}{2\pi j}\int_{\gamma_{1\eta}}\frac{Y_{11}(\eta')[V_{1+}(\eta')+V_{1\pi+}(-\eta')]+Y_{12}(\eta')e^{j\eta' s}[V_{2+}(\eta')+V_{2\pi+}(-\eta')]}{\eta'-\eta}d\eta' \quad (61)$$

Let us consider separately the integrand for each voltage unknown. Starting from the contribution of $V_{1+}(\eta)$, since

$$\frac{1}{2\pi j}\int_{\gamma_{2\eta}}\frac{Y_{11}(\eta)V_{1+}(\eta')}{\eta'-\eta}d\eta' = -Y_{11}(\eta)V_{1+}^{ns}(\eta) \quad (62)$$

$$\begin{aligned}&\tfrac{1}{2\pi j}\int_{\gamma_{1\eta}}\tfrac{Y_{11}(\eta')V_{1+}(\eta')}{\eta'-\eta}d\eta' - \tfrac{1}{2\pi j}\int_{\gamma_{2\eta}}\tfrac{Y_{11}(\eta)V_{1+}(\eta')}{\eta'-\eta}d\eta' = \\ &= Y_{11}(\eta)V_{1+}(\eta) + \tfrac{1}{2\pi j}\int_{-\infty}^{\infty}\tfrac{(Y_{11}(\eta')-Y_{11}(\eta))V_{1+}(\eta')}{\eta'-\eta}d\eta'\end{aligned} \quad (63)$$

we have

$$\begin{aligned}&\tfrac{1}{2\pi j}\int_{\gamma_{1\eta}}\tfrac{Y_{11}(\eta')V_{1+}(\eta')}{\eta'-\eta}d\eta' = Y_{11}(\eta)V_{1+}(\eta) + \\ &+\tfrac{1}{2\pi j}\int_{-\infty}^{\infty}\tfrac{(Y_{11}(\eta')-Y_{11}(\eta))V_{1+}(\eta')}{\eta'-\eta}d\eta' - Y_{11}(\eta)V_{1+}^{ns}(\eta)\end{aligned} \quad (64)$$

Focusing on the contribution of $V_{2+}(\eta)$ in (61) (similarly to what has been reported for $V_{1+}(\eta)$), using (14), since

$$\frac{1}{2\pi j}\int_{\gamma_{2\eta}}\frac{Y_{12}(\eta)V_{2+}(\eta')e^{j\eta s}}{\eta'-\eta}d\eta' = -Y_{12}(\eta)V_{2+}^{ns}(\eta)e^{j\eta s} \quad (65)$$

$$\frac{1}{2\pi j}\int\limits_{\gamma_{1\eta}}\frac{Y_{12}(\eta')V_{2+}(\eta')e^{j\eta' s}}{\eta'-\eta}d\eta'-\frac{1}{2\pi j}\int\limits_{\gamma_{2\eta}}\frac{Y_{12}(\eta)V_{2+}(\eta')e^{j\eta s}}{\eta'-\eta}d\eta'=$$
$$=Y_{12}(\eta)V_{2+}(\eta)e^{j\eta s}+\frac{1}{2\pi j}\int\limits_{-\infty}^{\infty}\frac{(Y_{12}(\eta')e^{j\eta' s}-Y_{12}(\eta)e^{j\eta s})V_{2+}(\eta')}{\eta'-\eta}d\eta' \tag{66}$$

we have

$$\frac{1}{2\pi j}\int\limits_{\gamma_{1\eta}}\frac{Y_{12}(\eta')V_{2+}(\eta')e^{j\eta' s}}{\eta'-\eta}d\eta'=Y_{12}(\eta)V_{2+}(\eta)e^{j\eta s}+$$
$$+\frac{1}{2\pi j}\int\limits_{-\infty}^{\infty}\frac{(Y_{12}(\eta')e^{j\eta' s}-Y_{12}(\eta)e^{j\eta s})V_{2+}(\eta')}{\eta'-\eta}d\eta'-Y_{12}(\eta)V_{2+}^{ns}(\eta)e^{j\eta s} \tag{67}$$

For what concerns the contribution of $V_{1\pi+}(-\eta)$ in (61), recalling $V_{1\pi+}^{ns}(\eta)=0$ and using (14), since

$$\frac{1}{2\pi j}\int\limits_{\gamma_{1\eta}}\frac{Y_{11}(\eta)V_{1\pi+}(-\eta')}{\eta'-\eta}d\eta'=0 \tag{68}$$

we have

$$\frac{1}{2\pi j}\int\limits_{\gamma_{1\eta}}\frac{Y_{11}(\eta')V_{1\pi+}(-\eta')}{\eta'-\eta}d\eta'=\frac{1}{2\pi j}\int\limits_{-\infty}^{\infty}\frac{(Y_{11}(\eta)-Y_{11}(-\eta'))V_{1\pi+}(\eta')}{\eta'+\eta}d\eta' \tag{69}$$

Considering the contribution of $V_{2\pi+}(\eta)$ in (61) (similarly to what has been reported for $V_{1\pi+}(\eta)$), recalling $V_{2\pi+}^{ns}(\eta)=0$ and using (14), since

$$\frac{1}{2\pi j}\int\limits_{\gamma_{1\eta}}\frac{Y_{12}(\eta)V_{2\pi+}(-\eta')e^{j\eta s}}{\eta'-\eta}d\eta'=0 \tag{70}$$

we have

$$\frac{1}{2\pi j}\int\limits_{\gamma_{1\eta}}\frac{Y_{12}(\eta')V_{2\pi+}(-\eta')e^{j\eta' s}}{\eta'-\eta}d\eta'=$$
$$=\frac{1}{2\pi j}\int\limits_{-\infty}^{\infty}\frac{(Y_{12}(\eta)e^{j\eta s}-Y_{12}(-\eta')e^{-j\eta' s})V_{2\pi+}(\eta')}{\eta'+\eta}d\eta' \tag{71}$$

The final regularized integral representation of the 1st eq. in (20) is given by equating (60) to (61) with the help of (64),(67),(69),(71):

$$-I_{1+}(\eta)=\mathcal{Y}_{e11}[V_{1+}]+\mathcal{Y}_{e12}[V_{2+}]+\mathcal{Y}_{e13}[V_{1\pi+}]+\mathcal{Y}_{e14}[V_{2\pi+}]+I_{sce1}(\eta) \tag{72}$$

where the η dependence of the voltages is omitted.

In (72) we have used network notation where the algebraic-integral operator admittances $\mathcal{Y}_{e1j}$, $j=1,2,3,4$ have the following explicit forms:

$$\begin{aligned}
\mathcal{Y}_{e11}[V_{1+}]&=Y_{11}(\eta)V_{1+}(\eta)+\tfrac{1}{2\pi j}\int\limits_{-\infty}^{\infty}y_{e11}(\eta,\eta')V_{1+}(\eta')d\eta'\\
\mathcal{Y}_{e12}[V_{2+}]&=Y_{12}(\eta)V_{2+}(\eta)e^{j\eta s}+\tfrac{1}{2\pi j}\int\limits_{-\infty}^{\infty}y_{e12}(\eta,\eta')V_{2+}(\eta')d\eta'\\
\mathcal{Y}_{e13}[V_{1\pi+}]&=\tfrac{1}{2\pi j}\int\limits_{-\infty}^{\infty}y_{e13}(\eta,\eta')V_{1\pi+}(\eta')d\eta'\\
\mathcal{Y}_{e14}[V_{2\pi+}]&=\tfrac{1}{2\pi j}\int\limits_{-\infty}^{\infty}y_{e14}(\eta,\eta')V_{2\pi+}(\eta')d\eta'
\end{aligned} \tag{73}$$

with

$$\begin{aligned}
y_{e11}(\eta,\eta')&=\tfrac{Y_{11}(\eta')-Y_{11}(\eta)}{\eta'-\eta}\\
y_{e12}(\eta,\eta')&=\tfrac{Y_{12}(\eta')e^{j\eta' s}-Y_{12}(\eta)e^{+j\eta s}}{\eta'-\eta}\\
y_{e13}(\eta,\eta')&=\tfrac{Y_{11}(\eta)-Y_{11}(-\eta')}{\eta'+\eta}\\
y_{e14}(\eta,\eta')&=\tfrac{Y_{12}(\eta)e^{j\eta s}-Y_{12}(-\eta')e^{-j\eta' s}}{\eta'+\eta}
\end{aligned} \tag{74}$$

In (72) we have also defined $I_{sce1}(\eta)$ that collects all the non-standard GO singularities that are extracted in (64),(67),(69),(71):

$$I_{sce1}(\eta)=I_{1+}^{ns}(\eta)+Y_{11}(\eta)V_{1+}^{ns}(\eta)+Y_{12}(\eta)e^{j\eta s}V_{2+}^{ns}(\eta) \tag{75}$$

Using network notation $I_{sce1}(\eta)$ is a short-circuit current at port 1, while $V_{1+}(\eta)$ and $I_{1+}(\eta)$ are the voltage and current at the same port. $V_{2+}(\eta)$, $V_{1\pi+}(\eta)$, $V_{2\pi+}(\eta)$ are respectively the voltage at port 2,3,4. Eq. (72) represents the first out of four constitutive relations of the 4-port model that relates the plus unknowns defined on the layer.

By repeating the same procedure to the 2nd eq of (20) and to the modified eqs. of (20) while interchanging η with $-\eta$, we get the complete integral representation of the layer. The final representation is reported in (76). In (76) algebraic-integral operator admittances show repetitions almost in a symmetrical form. To complete the definition of kernels in (76) we report the algebraic-integral operator admittances of the second row:

$$\begin{aligned}
\mathcal{Y}_{e21}[V_{1+}]&=Y_{21}(\eta)V_{1+}(\eta)e^{-j\eta s}+\tfrac{1}{2\pi j}\int\limits_{-\infty}^{\infty}y_{e21}(\eta,\eta')V_{1+}(\eta')d\eta'\\
\mathcal{Y}_{e22}[V_{2+}]&=Y_{22}(\eta)V_{2+}(\eta)+\tfrac{1}{2\pi j}\int\limits_{-\infty}^{\infty}y_{e22}(\eta,\eta')V_{2+}(\eta')d\eta'\\
\mathcal{Y}_{e23}[V_{1\pi+}]&=\tfrac{1}{2\pi j}\int\limits_{-\infty}^{\infty}y_{e23}(\eta,\eta')V_{1\pi+}(\eta')d\eta'\\
\mathcal{Y}_{e24}[V_{2\pi+}]&=\tfrac{1}{2\pi j}\int\limits_{-\infty}^{\infty}y_{e24}(\eta,\eta')V_{2\pi+}(\eta')d\eta'
\end{aligned} \tag{77}$$

with

$$\begin{aligned}
y_{e21}(\eta,\eta')&=\tfrac{Y_{12}(\eta')e^{-j\eta' s}-Y_{12}(\eta)e^{-j\eta s}}{\eta'-\eta}\\
y_{e22}(\eta,\eta')&=\tfrac{Y_{22}(\eta')-Y_{22}(\eta)}{\eta'-\eta}\\
y_{e23}(\eta,\eta')&=\tfrac{Y_{21}(\eta)e^{-j\eta s}-Y_{21}(-\eta')e^{j\eta' s}}{\eta'+\eta}\\
y_{e24}(\eta,\eta')&=\tfrac{Y_{22}(\eta)-Y_{22}(-\eta')}{\eta'+\eta}
\end{aligned} \tag{78}$$

To complete the definition of source term in (76) we report:

$$\begin{aligned}
I_{sce2}(\eta)&=-I_{2+}^{ns}(\eta)+Y_{22}(\eta)V_{2+}^{ns}(\eta)+Y_{21}(\eta)e^{-j\eta s}V_{1+}^{ns}(\eta)\\
I_{sce3}(\eta)&=-Y_{11}(\eta)V_{1+}^{ns}(-\eta)-I_{1+}^{ns}(-\eta)-Y_{12}(\eta)e^{-j\eta s}V_{2+}^{ns}(-\eta)\\
I_{sce4}(\eta)&=-Y_{22}(\eta)V_{2+}^{ns}(-\eta)+I_{2+}^{ns}(-\eta)-Y_{21}e^{j\eta s}V_{1+}^{ns}(-\eta)
\end{aligned} \tag{79}$$

Note that (79) are valid with the assumption that the plane wave source originates from region A, otherwise non-standard terms arise also from $\pi+$ unknowns. As anticipated, (76) is interpreted as a generalized Norton model with four ports. Fig. 4 shows a pictorial illustration of the model.

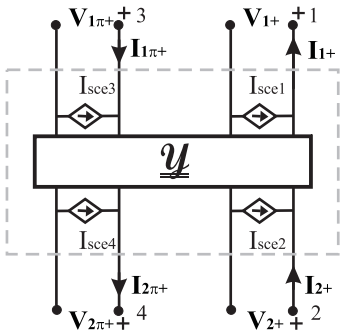

Fig. 4: Generalized Norton equivalent network model of region E corresponding to (76).

$$\begin{pmatrix} -I_{1+}(\eta) \\ I_{2+}(\eta) \\ I_{1\pi+}(\eta) \\ -I_{2\pi+}(\eta) \end{pmatrix} = \begin{bmatrix} \mathcal{Y}_{e11}[\cdot] & \mathcal{Y}_{e12}[\cdot] & \mathcal{Y}_{e13}[\cdot] & \mathcal{Y}_{e14}[\cdot] \\ \mathcal{Y}_{e21}[\cdot] & \mathcal{Y}_{e22}[\cdot] & \mathcal{Y}_{e23}[\cdot] & \mathcal{Y}_{e24}[\cdot] \\ \mathcal{Y}_{e13}[\cdot] & \mathcal{Y}_{e23}[\cdot] & \mathcal{Y}_{e11}[\cdot] & \mathcal{Y}_{e21}[\cdot] \\ \mathcal{Y}_{e14}[\cdot] & \mathcal{Y}_{e24}[\cdot] & \mathcal{Y}_{e12}[\cdot] & \mathcal{Y}_{e22}[\cdot] \end{bmatrix} \begin{pmatrix} V_{1+}(\eta) \\ V_{2+}(\eta) \\ V_{1\pi+}(\eta) \\ V_{2\pi+}(\eta) \end{pmatrix} + \begin{pmatrix} -I_{sce1}(\eta) \\ -I_{sce2}(\eta) \\ -I_{sce3}(\eta) \\ -I_{sce4}(\eta) \end{pmatrix} \tag{76}$$

C. FIEs of the Problem and Solution

The constitutive relations of the five regions reported as integral representations in (35),(41),(47),(54) and (76) (sketched in Figs. 3-4) relate plus current unknowns to plus voltage unknowns. Note that the models are obtained once and for all. The complete problem (Fig. 1) is modelled via a connected network, see Fig.5, amenable of simplification by substitution in terms of voltages as in circuit theory. The elimination of plus currents allows to obtain a system of integral equations in terms of plus voltages $\mathbf{V}_+(\eta) = [V_{1+}(\eta), V_{2+}(\eta), V_{1\pi+}(\eta), V_{2\pi+}(\eta)]'$ whose kernel is of Fredholm type of second kind due to the regularization procedure applied in the previous sub-sections. In normal form we obtain

$$\mathbf{V}_+(\eta) + \frac{1}{2\pi j}\int_{-\infty}^{\infty} \mathbf{M}(\eta,\eta')\cdot\mathbf{V}_+(\eta')d\eta' = \mathbf{N}(\eta) \tag{80}$$

for $\eta \in \mathbb{R}$ where the kernel is

$$\mathbf{M}(\eta,\eta') = \mathbf{Z}_t(\eta)\cdot\mathbf{Y_t}(\eta,\eta') \tag{81}$$

with $\mathbf{Y}_t(\eta,\eta')$ reported in (82) and

$$\mathbf{Z}_t(\eta) = \begin{vmatrix} Z^e(\eta) & e^{j\eta s}Z^e_m(\eta) & 0 & 0 \\ e^{-j\eta s}Z^e_m(\eta) & Z^e(\eta) & 0 & 0 \\ 0 & 0 & Z^e(\eta) & e^{j\eta s}Z^e_m(\eta) \\ 0 & 0 & e^{-j\eta s}Z^e_m(\eta) & Z^e(\eta) \end{vmatrix} \tag{83}$$

$$Z^e(\eta) = \frac{k\,Z_o}{2\xi(\eta)}, \qquad Z^e_m(\eta) = \frac{k\,Z_o e^{-j\xi(\eta)d}}{2\xi(\eta)} \tag{84}$$

The source term $\mathbf{N}(\eta)$ is

$$\mathbf{N}(\eta) = \mathbf{Z}_t(\eta)\cdot\begin{vmatrix} I_{sca}(\eta)+I_{sce1}(\eta) \\ I_{scc}(\eta)+I_{sce2}(\eta) \\ I_{sce3}(\eta) \\ I_{sce4}(\eta) \end{vmatrix} \tag{85}$$

A detailed discussion on (80) allows to ascertain that, in absence of regions filled by materials different from the free space, the singularities of $\mathbf{V}_+(\eta)$ are the branch point $\eta = k$ and the poles $\eta_{go} = -k\cos(\varphi_{go})$ arisen from GO contributions. While classical factorization requires some mathematical skill and it is only available in relatively very few special cases (geometry and source), the kernels $\mathbf{M}(\eta,\eta')$ of (80) involve simple mathematical functions. Simple numerical quadratures, such as sample and hold, allow to obtain approximate solutions of Fredholm type of second kind [87] as (80).

Taking into account the Meixner condition near the edges, the asymptotic behavior of the unknowns of each components of $\mathbf{V}_+(\eta)$ for $\eta \to \infty$ is $o(\eta^{-1-\nu})$ with $\nu > 0$ [88]. The fast convergence of the unknowns allows to estimate the integral in (80) on a limited spectral band.

To make a rigorous mathematical discussion and suggest other properties and/or solution techniques of (80), we use functional analysis. In particular it is possible to show that in the generalized Hilbert space $L_2(\mathbb{R},\mu(\eta))$ where $\mu(\eta)$ is a suitable weight with $\mu(\eta) = O(\eta^{-1/2})$, the matrix kernel $\mathbf{M}(\eta,\eta')$ is a compact operator [6],[55].

We note that when singularities are near the integration line, in order to obtain fast convergence of (80), we need to warp the integration line on a suitable path $v(u)$ that keeps the singularities at a suitable distance. We observe that in our problem the singularities of the kernel and of the source term are located in the 2nd and 4th quadrant (see also Figs. 13-14 of [16]), therefore we warp the real axis into the line $B_\theta : v(u) = ue^{j\theta}$, $u \in \mathbb{R}, 0 < \theta < \pi/2$ [22] that does not capture singularities of the integrand. Both observation point η and integration point η' lie on B_θ, thus (80) becomes

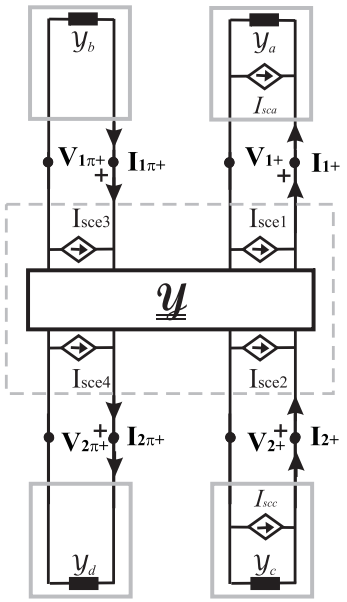

Fig. 5: Network equivalent model of the double PEC wedge problem.

$$\mathbf{V}_+(\eta) + \int_{B_\theta} \mathbf{M}(\eta,\eta')\cdot\mathbf{V}_+(\eta')d\eta' = \mathbf{N}(\eta), \eta \in B_\theta \tag{86}$$

Due to the presence of exponential factors $e^{j\eta' s}$ in $\mathbf{M}(\eta,\eta')$, the closure at infinity between the real axis and B_θ with arcs is possible only if $0 < \tan\theta < d/|s|$. However the solution of the FIE (86) on the line B_θ is efficient also for small values of θ that corresponds to small values of d with respect to $|s|$. To estimate (86) we apply simple sample and hold quadrature in a limited interval where A and h are respectively the truncation and the step parameters of integration such that $A/h \in \mathbb{N}$:

$$\mathbf{V}_+(v(u)) + h\sum_{i=-A/h}^{A/h} \mathbf{M}(v(u), v(h\,i))\cdot\mathbf{V}_+(v(h\,i))v'(h\,i) = \mathbf{N}(v(u)) \tag{87}$$

By sampling (87) at $u = hi$ with $i = -A/h..A/h$ we obtain a linear system with unknowns $\mathbf{V}_+(v(h\,i))$, whose solution allows to reconstruct an approximate version of $\mathbf{V}_+(\eta)$ through

$$\mathbf{V}_+(\eta) = -h\sum_{i=-A/h}^{A/h} \mathbf{M}(\eta, v(h\,i))\cdot\mathbf{V}_+(v(h\,i))v'(h\,i) + \mathbf{N}(\eta) \tag{88}$$

This representation is valid for observation points $\eta \in B_\theta$ (with $\eta' \in B_\theta$) and by analytic continuation also for a strip near $\eta \in B_\theta$ until observation point η crosses one of the singularity lines of $\mathbf{M}(\eta,\eta')$, see Section IV-A for definition. Finally (35),(41),(47),(54) or (76) with discretized integrals

$$\mathbf{Y}_t(\eta,\eta') = \begin{vmatrix} y_a(\eta,\eta')+y_{e11}(\eta,\eta') & y_{e12}(\eta,\eta') & y_{e13}(\eta,\eta') & y_{e14}(\eta,\eta') \\ y_{e21}(\eta,\eta') & y_b(\eta,\eta')+y_{e22}(\eta,\eta') & y_{e23}(\eta,\eta') & y_{e24}(\eta,\eta') \\ y_{e13}(\eta,\eta') & y_{e23}(\eta,\eta') & y_c(\eta,\eta')+y_{e11}(\eta,\eta') & y_{e21}(\eta,\eta') \\ y_{e14}(\eta,\eta') & y_{e24}(\eta,\eta') & y_{e12}(\eta,\eta') & y_d(\eta,\eta')+y_{e22}(\eta,\eta') \end{vmatrix} \quad (82)$$

allow to obtain $\mathbf{I}_+(\eta) = [I_{1+}(\eta), I_{2+}(\eta), I_{1\pi+}(\eta), I_{2\pi+}(\eta)]'$ in terms of the samples $\mathbf{V}_+(v(h\,i))$.

V. Analytic Continuation

In the following we combine two different techniques to obtain the analytic extension of the approximate solution (88). The first is based on the introduction of the angular complex plane w and thus the representation of the GWHEs in this complex plane that yields recursive equations. The second is related to contour warping of the representation given in (80) and (86) by taking care of singularity lines using the Cauchy's integral formula as described in Section IV-A.

The recursive equations strategy has been effectively applied in several scattering problems dealing with isolated wedges (see for example [16]-[21]) or dealing with complex structures constituted of layers and wedges (see for example [53]-[57]).

In order to analytically extend an initial spectrum coming from the approximate solution of FIEs, it is convenient to define the spectrum in the angular complex plane w through the mapping (89) (see the inverse mapping in [16]).

$$\eta = -k\cos w \quad (89)$$

From here on we introduce the following notations to indicate the spectra in the w-plane:

$$\hat{F}_+(w) = F_+(-k\cos w), \qquad \hat{F}_d(w) = \sin w \hat{F}_+(w) \quad (90)$$

A fundamental property of the plus functions in w-plane is that they are even function of w [14], i.e.

$$\hat{F}_+(w) = \hat{F}_+(-w), \qquad \hat{F}_d(-w) = -\hat{F}_d(w) \quad (91)$$

This property is important to eliminate the (generalized) minus functions in the GWHEs while represented in w plane.

The procedure to obtain recursive equations that allows to analytically extend the spectra of plus unknowns $\hat{V}_{1d}(w), \hat{I}_{1+}(w), \hat{V}_{2d}(w), \hat{I}_{2+}(w), \hat{V}_{1\pi d}(w), \hat{I}_{1\pi+}(w), \hat{V}_{2\pi d}(w), \hat{I}_{2\pi+}(w)$ is based on the following steps using algebraic manipulations: 1) represent the GWHEs (15), (20) and modified (20) ($\eta \to -\eta$) in w plane, 2) using symmetry of even functions in w and shifting w we eliminate the currents on the faces in (15) and one of the two currents in (20) and modified (20), 3) the system of equation of point 2 allows to get each plus unknown in terms of the all plus unknowns with argument $(2\pi + w)$ or $(2\Phi_f + w)$ $(f = a, b, c, d)$. The results are the expressions (92) that allow analytic extension of the spectra for any w from an initial spectra coming from (88) and represented in w plane. Note that the spectra of regions B and D are decoupled from the spectra of regions A and C in (92).

To effectively implement the analytic continuation via (92) and (91), we need an initial spectra of voltage/current unknowns valid at least in the strip $-\pi < Re[w] < 0$ of w complex plane. In fact from (92) and (91) we get recursive equations for plus functions of the following kind:

$$F_+(w) = \begin{cases} F_+(-w) & w > 0 \\ F_+^{num}(w) & -\pi \le w \le 0 \\ \text{select appropriate (92)} & w < -\pi \end{cases} \quad (93)$$

where $F_+^{num}(w)$ is the initial approximate spectrum coming from the solution of FIEs. Similar expressions can be easily derived for odd functions d using (92).

However the validity strip of the initial approximate spectra (88) (and related currents) can be limited in a strip smaller than $-\pi < Re[w] < 0$ by the presence of singularity lines $(p_n^{\Phi_f}(\eta),\ f = a, b, c, d)$ of the kernel $\mathbf{M}(\eta,\eta')$, in particular when the observation point crosses singularity lines not captured in the derivation of (88) (see also Section IV-A). In w-plane the singularity lines assume simple forms. They are parallel to the image of the integration contour B_θ (86): $B_\theta^w : w' = -\arccos(-ve^{j\theta})$, $v \in \mathbb{R}$. For an angular region of aperture Φ_a, they are defined respectively in α, η, w planes by

$$\begin{aligned} &\alpha(\eta) = \alpha(\eta'),\ \eta \neq \eta' \\ &\eta' = p_n^{\Phi_a}(\eta) = \eta\cos(2n\Phi_a) - \xi(\eta)\sin 2n\Phi_a,\ \eta \neq \eta' \\ &w = -w' + 2n\Phi_a,\ w' \neq w \end{aligned} \quad (94)$$

with $\eta' \in B_\theta$, $w' \in B_\theta^w$ and $n \in \mathbb{N}_0$, thus the singularity lines are easily countable and located in w plane.

In general, to get a representation with extended validity at least in $-\pi < Re[w] < 0$ we need to locate accurately the singularity lines and to extract correction terms as described in Section IV-A and [55].

VI. Diffraction and Far Field

The pairs of axial spectral unknowns $\{\hat{V}_{1d}(w), \hat{I}_{1+}(w)\}$, $\{\hat{V}_{1\pi d}(w), \hat{I}_{1\pi+}(w)\}$, $\{\hat{V}_{2d}(w), \hat{I}_{2+}(w)\}$, $\{\hat{V}_{2\pi d}(w), \hat{I}_{2\pi+}(w)\}$ provide the Laplace transforms in the w plane of the electromagnetic field respectively for $\{y = 0, x > 0\}$, $\{y = 0, x < 0\}$, $\{y_2 = 0, x_2 > 0\}$, $\{y_2 = 0, x_2 < 0\}$ that are the interfaces towards regions A,B,C,D. Given the axial spectra we can obtain the spectra in any azimuthal direction in the regions. In the following we focus the attention on the angular region A, and then we extrapolate the results for angular regions B,C,D from it.

With reference to angular region A, the spectra for any direction φ is obtained through the expressions [89]:

$$\begin{cases} \hat{V}_{1d}(w,\varphi) = \frac{Z_o(\hat{I}_{1+}(w-\varphi)-\hat{I}_{1+}(w+\varphi))+\hat{V}_{1d}(w-\varphi)+\hat{V}_{1d}(w+\varphi)}{2} \\ I_{1+}(w,\varphi) = \frac{Z_o(\hat{I}_{1+}(w-\varphi)+\hat{I}_{1+}(w+\varphi))+\hat{V}_{1d}(w-\varphi)-\hat{V}_{1d}(w+\varphi)}{2} \end{cases} \quad (95)$$

for $0 \le \varphi \le \Phi_a$, where $\hat{V}_{1d}(w,\varphi) = \sin w \hat{V}_{1+}(w,\varphi) = \sin w V_{1+}(-k\cos w, \varphi)$ and $\hat{I}_{1+}(w,\varphi) = I_{1+}(-k\cos w, \varphi)$ that are respectively an odd and an even function of w.

The exact total field for $0 < \varphi < \Phi_a$ is given by the following inverse Laplace-w transforms:

$$\begin{aligned} E_z(\rho,\varphi) &= \tfrac{k}{2\pi}\textstyle\int_{\lambda(B_r)} \hat{V}_{1+}(w,\varphi) e^{jk\rho\cos w}\sin w dw \\ H_\rho(\rho,\varphi) &= \tfrac{k}{2\pi}\textstyle\int_{\lambda(B_r)} \hat{I}_{1+}(w,\varphi) e^{jk\rho\cos w}\sin w dw \end{aligned} \quad (96)$$

where $\lambda(B_r)$ is the mapping of the Bromwich B_r contour of the η-plane into the w-plane, see for example [20] for details.

By applying the steepest descent path (SDP) method to equations (96), the total field is composed as in (97):

$$E_z(\rho,\varphi) = E_z^g(\rho,\varphi) + E_z^d(\rho,\varphi) \quad (97)$$

where $E_z^g(\rho,\varphi)$ (98) and $E_z^d(\rho,\varphi)$ (99) are respectively the contribution related to GO poles and the integral along the SDP that is the diffracted component

$$
\begin{aligned}
\hat{V}_{1d}(w) &= \tfrac{1}{2}\Big[-Z_o\hat{I}_{1+}(2\pi+w)+Z_o\hat{I}_{1+}(w+2\Phi_a)+\hat{V}_{1d}(2\pi+w)-\hat{V}_{1d}(w+2\Phi_a)+\\
&\quad -e^{-jks\cos(w)+jkd\sin(w)}\Big(-Z_o\hat{I}_{2+}(2\pi+w)+Z_o\hat{I}_{2+}(w+2\Phi_c)+\hat{V}_{2d}(2\pi+w)+\hat{V}_{2d}(w+2\Phi_c)\Big)\Big]\\
\hat{I}_{1+}(w) &= \tfrac{1}{2Z_o}\Big[Z_o\hat{I}_{1+}(2\pi+w)+Z_o\hat{I}_{1+}(w+2\Phi_a)-\hat{V}_{1d}(2\pi+w)-\hat{V}_{1d}(w+2\Phi_a)+\\
&\quad -e^{-jks\cos(w)+jkd\sin(w)}\Big(Z_o\hat{I}_{2+}(2\pi+w)-Z_o\hat{I}_{2+}(w+2\Phi_c)-\hat{V}_{2d}(2\pi+w)-\hat{V}_{2d}(w+2\Phi_c)\Big)\Big]\\
\hat{V}_{2d}(w) &= \tfrac{1}{2}\Big[Z_o\hat{I}_{2+}(2\pi+w)-Z_o\hat{I}_{2+}(w+2\Phi_c)+\hat{V}_{2d}(2\pi+w)-\hat{V}_{2d}(w+2\Phi_c)+\\
&\quad -e^{jks\cos(w)+jkd\sin(w)}\Big(Z_o\hat{I}_{1+}(2\pi+w)-Z_o\hat{I}_{1+}(w+2\Phi_a)+\hat{V}_{1d}(2\pi+w)+\hat{V}_{1d}(w+2\Phi_a)\Big)\Big]\\
\hat{I}_{2+}(w) &= \tfrac{1}{2Z_o}\Big[Z_o\hat{I}_{2+}(2\pi+w)+Z_o\hat{I}_{2+}(w+2\Phi_c)+\hat{V}_{2d}(2\pi+w)+\hat{V}_{2d}(w+2\Phi_c)+\\
&\quad -e^{jks\cos(w)+jkd\sin(w)}\Big(Z_o\hat{I}_{1+}(2\pi+w)-Z_o\hat{I}_{1+}(w+2\Phi_a)+\hat{V}_{1d}(2\pi+w)+\hat{V}_{1d}(w+2\Phi_a)\Big)\Big]\\
\hat{V}_{1\pi d}(w) &= \tfrac{1}{2}\Big[Z_o\hat{I}_{1\pi+}(2\pi+w)-Z_o\hat{I}_{1\pi+}(w+2\Phi_b)+\hat{V}_{1\pi d}(2\pi+w)-\hat{V}_{1\pi d}(w+2\Phi_b)+\\
&\quad -e^{jks\cos(w)+jkd\sin(w)}\Big(Z_o\hat{I}_{2\pi+}(2\pi+w)-Z_o\hat{I}_{2\pi+}(w+2\Phi_d)+\hat{V}_{2\pi d}(2\pi+w)+\hat{V}_{2\pi d}(w+2\Phi_d)\Big)\Big]\\
\hat{I}_{1\pi+}(w) &= \tfrac{1}{2Z_o}\Big[Z_o\hat{I}_{1\pi+}(2\pi+w)+Z_o\hat{I}_{1\pi+}(w+2\Phi_b)+\hat{V}_{1\pi d}(2\pi+w)+\hat{V}_{1\pi d}(w+2\Phi_b)+\\
&\quad -e^{jks\cos(w)+jkd\sin(w)}\Big(Z_o\hat{I}_{2\pi+}(2\pi+w)-Z_o\hat{I}_{2\pi+}(w+2\Phi_d)+\hat{V}_{2\pi d}(2\pi+w)+\hat{V}_{2\pi d}(w+2\Phi_d)\Big)\Big]\\
\hat{V}_{2\pi d}(w) &= \tfrac{1}{2}\Big[-Z_o\hat{I}_{2\pi+}(2\pi+w)+Z_o\hat{I}_{2\pi+}(w+2\Phi_d)+\hat{V}_{2\pi d}(2\pi+w)-\hat{V}_{2\pi d}(w+2\Phi_d)+\\
&\quad -e^{-jks\cos(w)+jkd\sin(w)}\Big(-Z_o\hat{I}_{1\pi+}(2\pi+w)+Z_o\hat{I}_{1\pi+}(w+2\Phi_b)+\hat{V}_{1\pi d}(2\pi+w)+\hat{V}_{1\pi d}(w+2\Phi_b)\Big)\Big]\\
\hat{I}_{2\pi+}(w) &= \tfrac{1}{2Z_o}\Big[Z_o\hat{I}_{2\pi+}(2\pi+w)+Z_o\hat{I}_{2\pi+}(w+2\Phi_d)-\hat{V}_{2\pi d}(2\pi+w)-\hat{V}_{2\pi d}(w+2\Phi_d)+\\
&\quad -e^{-jks\cos(w)+jkd\sin(w)}\Big(Z_o\hat{I}_{1\pi+}(2\pi+w)-Z_o\hat{I}_{1\pi+}(w+2\Phi_b)-\hat{V}_{1\pi d}(2\pi+w)-\hat{V}_{1\pi d}(w+2\Phi_b)\Big)\Big]
\end{aligned}
\tag{92}
$$

$$E_z^g(\rho,\varphi) = -jk\sum_i \mathrm{Res}[\hat{\mathrm{V}}_{1\mathrm{d}}(\mathrm{w},\varphi)]_{\mathrm{w_i}(\varphi)}\ \mathrm{e}^{+\mathrm{jk}\rho\cos\mathrm{w_i}(\varphi)} \tag{98}$$

$$E_z^d(\rho,\varphi) = -\frac{ke^{-jk\rho}}{2\pi}\int_{\mathrm{SDP}}\hat{V}_{1d}(w,\varphi)e^{k\rho h(w)}dw \tag{99}$$

where $h(w)=k\rho(\cos w+1)$, $w_i(\varphi)=w_{oi}\pm\varphi$ and w_{oi} are the poles of the axial spectrum $\hat{V}_{1d}(w)$. As an alternative, classical GO considerations can be used to obtain the GO components. Since on the SDP $h(w)$ is a continuous real function, which rapidly goes to $-\infty$ toward the end points of the path, as $k\rho\to\infty$, the main contribution in (99) is located near the saddle point $-\pi$, thus the diffracted component can be approximated with the GTD component:

$$E_z^{gtd}(\rho,\varphi) = E_o\frac{e^{-j(k\rho+\frac{\pi}{4})}}{\sqrt{2\pi k\rho}}D_A(\varphi,\varphi_o) \tag{100}$$

$$D_A(\varphi,\varphi_o) = \frac{-k\hat{V}_{1d}(-\pi,\varphi)}{jE_o} \tag{101}$$

This expression makes the importance of the analytic continuation of Section V clear. In fact, to estimate $\hat{V}_{1d}(-\pi,\varphi)$ in $0<\varphi<\Phi_a$, we need the axial spectra defined in the range $-\pi-\Phi_a<w<-\pi+\Phi_a$, see (95).

Uniform expressions of the total far field $E_z^{tot}=E_z^g+E_z^{utd}$ are obtained via the Uniform Theory of Diffraction (UTD), which removes caustics of GTD at shadow boundaries [90]:

$$E_z^{utd}(\rho,\varphi) = E_o\frac{e^{-j\left(k\rho+\frac{\pi}{4}\right)}}{\sqrt{2\pi k\rho}}C_A(\varphi,\varphi_o) \tag{102}$$

$$C_A(\varphi,\varphi_o) = D_A(\varphi,\varphi_o)+\sum_{go}\Gamma_{go}\frac{1-F\left(2k\rho\cos^2\frac{\varphi-\varphi_{go}-\pi}{2}\right)}{\cos\frac{\varphi-\varphi_{go}-\pi}{2}} \tag{103}$$

where Γ_{go} are the coefficients of the GO components of incoming direction φ_{go} and the function $F(z)$ is the Kouyoumjian-Pathak transition function defined in [90] and its application in the framework of WH formulations is reported in (63) of [16].

Following the same procedure we obtain similar expressions for the other angular regions. In particular we observe that for regions B and D (while illuminating the structure from region A with a plane wave) the spectra do not contain any GO poles since no GO component shows infinite support. In this case the asymptotic evaluation of fields contains only a regular (no caustics) GTD component due to the integral along the SDP.

For region B $\pi-\Phi_b<\varphi<\pi$ ($\varphi_1=\pi-\varphi$), we have [54]:

$$E_z^d(\rho,\varphi_1) = -\frac{ke^{-jk\rho}}{2\pi}\int_{\mathrm{SDP}}\hat{V}_{1\pi d}(w,\varphi_1)e^{k\rho h(w)}dw \tag{104}$$

$$\begin{cases}\hat{V}_{1\pi d}(w,\varphi_1)=\frac{Z_o(\hat{I}_{1\pi+}(w+\varphi_1)-\hat{I}_{1\pi+}(w-\varphi_1))+\hat{V}_{1\pi d}(w-\varphi_1)+\hat{V}_{1\pi d}(w+\varphi_1)}{2}\\ I_{1\pi+}(w,\varphi_1)=\frac{Z_o(\hat{I}_{1\pi+}(w-\varphi_1)+\hat{I}_{1\pi+}(w+\varphi_1))+\hat{V}_{1\pi d}(w+\varphi_1)-\hat{V}_{1\pi d}(w-\varphi_1)}{2}\end{cases} \tag{105}$$

that yields the GTD component:

$$E_z^{gtd}(\rho,\varphi_1) = E_o\frac{e^{-j(k\rho+\frac{\pi}{4})}}{\sqrt{2\pi k\rho}}D_B(\varphi_1,\varphi_o) \tag{106}$$

$$D_B(\varphi_1,\varphi_o) = \frac{-k\hat{V}_{1\pi d}(-\pi,\varphi_1))}{jE_o} \tag{107}$$

We recall that the asymptotic field for region A and B is computed with reference coordinate system centered in O, while for regions C and D is computed with reference coordinate system centered in O'' (see Fig. 1). To obtain the GTD diffraction coefficients and total field in regions C and D the expression obtained for A and B can respectively be used by substituting the spectral components defined at $y=0$ (labeled 1) with the ones defined at $y_2=0$ (labeled 2).

VII. Validation and Numerical Results

With reference to the problem of Fig. 1 at E_z polarization, in this Section we provide validations and numerical tests of the proposed method in relation to the geometrical and physical parameters: s, d, Φ_a, Φ_b, Φ_c, Φ_d, φ_o and $E_o=1V/m$ in (1). For the sake of brevity and with minimum impact, we impose $\Phi_d=0$ and $0<\varphi_o<\Phi_a$, thus the problem is reduced of 1 region and (80) can be simplified by eliminating the unknowns of region D, thus the system of equations is reduced from size 4 to size 3. In fact by rotation the structure of Fig. 1 can

be reduced to this case. Note that with this assumptions the source term $\mathbf{N}(\eta)$ (108) is reduced to three components

$$\mathbf{N}(\eta) = \mathbf{Z}_t(\eta) \cdot \left| \begin{array}{c} I_{sca}(\eta) + I_{sce1}(\eta) \\ I_{scc}(\eta) + I_{sce2}(\eta) \\ I_{sce3}(\eta) \end{array} \right| \tag{108}$$

As stated in Section II, to meet mathematical requirements of the WH technique small vanishing losses are assumed in the medium, and in the following numerical examples we assume $k = k' - j10^{-8}k'$. For computational purpose we have selected $k' = 1$. The analysis of problem for practical values of geometrical/electromagnetic parameters is obtainable by scaling the quantities according to [17], [57]. In particular a different value of k' (for example $k' = p$ such that $k_{new} = p(1 - j10^{-8})$) changes the computed spectrum $F_+(\eta)$ to $\frac{k}{k_{new}} F_+(\frac{k\eta}{k_{new}})$, and the distance d and s becomes respectively kd/k_{new} and ks/k_{new}. Note that in our formulation the dependence on d and s appears always as kd and ks thus all quantities are invariant for constant kd and ks.

In the following we make self-convergence tests and validation thorough an independent fully numerical solution obtained by a in-house code based on the Finite Element Method (FEM) embedding singular modelling [82] with the following setup: region truncated at a distance of $\rho = 12\lambda$ from the origin O with perfectly matched layer of cylindrical shape of depth $\lambda/2$ and discretization via quadratic triangular elements with max side length of $\lambda/10$. Although we have truncated the structure at a large distance from the origin in FEM, the truncation generates spurious diffraction/reflections that compromise the precision of this solution. On the contrary our semi-analytical method does not suffer of such limit and this phenomenon demonstrates its superiority for the analysis of infinite canonical problems with the only limit due to the computation of asymptotics.

Solutions are reported in terms of spectra, GTD coefficients, UTD fields, total far fields for validation, see Section VI for details. We recall that the proposed solution is obtained directly from the axial spectra of the complete problem and not using multiple steps of interaction among separated objects like in iterative physical optics or using multiple diffraction coefficients as in ray-tracing technique.

The proposed significant test case analyzes in depth a configuration of the double PEC wedge problem in free space. All the properties of our solution are given in terms of spectral quantities, diffraction coefficients, and total far fields. With reference to Fig. 1, the physical parameters of the problem in the selected test case are: $\Phi_a = 0.65\pi, \Phi_b = 0.3\pi, \Phi_c = 0.7\pi, k_r d = 2, k_r s = 3$ and $E_o = 1V/m, \varphi_o = 0.1\pi$ and $k = k' - jk''$ where $k', k'' > 0$ and $k''/k' = 10^{-8}$. According to GO, the E-polarized incident plane wave impinges on the wedges and generates reflections from face A and C respectively with azimuthal directions $\varphi_{RA} = -\pi + 2\Phi_a - \varphi_o = 0.2\pi$ and $\varphi_{RC} = +\pi - 2\Phi_c - \varphi_o = -0.5\pi$. While computing the solution of (86) we have selected $\theta = \pi/6$ such that $0 < \tan\theta < d/|s| = 2/3$.

In particular we note that in this test case, while computing (80)-(88), we need to consider the singularity line $p_1^{\Phi_b}(\eta)$, see discussion of (35). Moreover, in this test case, due to the presence of further singularity lines, the initial validity strip in

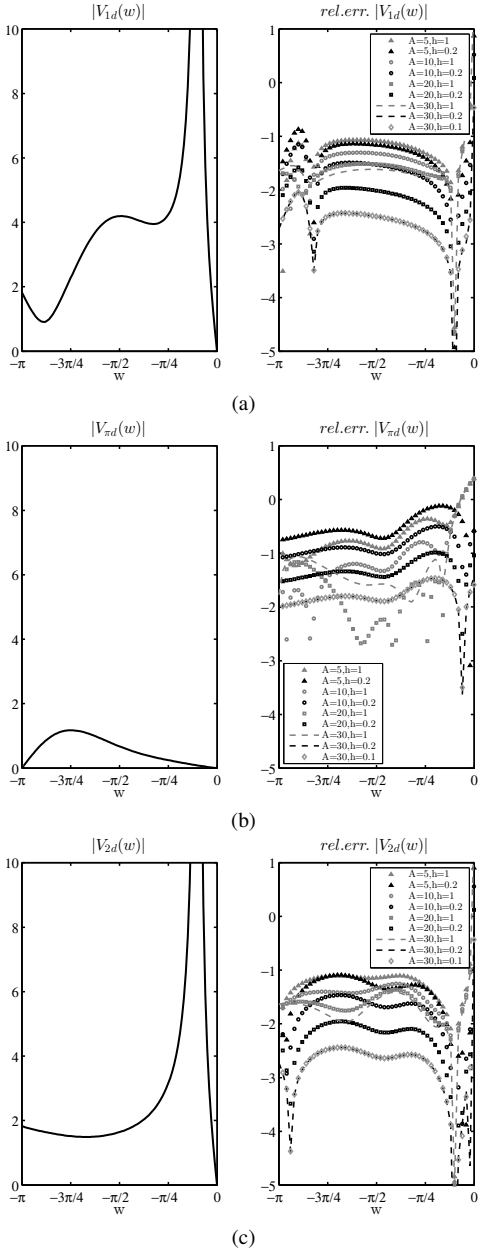

Fig. 6: Test Case. Convergence of spectral components. Left: plots of (a) $|V_{1d}(w)|$, (b) $|V_{1\pi d}(w)|$, (c) $|V_{2d}(w)|$ of the reference solution (integration parameters $A = 40, h = 0.1$) for $-\pi < w < 0$. Right: plots of the corresponding relative error in log_{10} scale of solution with various integration parameters A, h with respect to the reference solution.

w plane does not contain the segment $-\pi < w < 0$ useful for the application of recursive equations (93) with (92) to get the spectra for GTD computation (Section VI), i.e. $-\pi - \Phi_f < w < -\pi + \Phi_f$, $f = a, b, c$. Due to dependence of singularity lines on the aperture angles of the angular regions, while estimating the spectra for $-\pi < w < 0$ in this test case, we need to consider the singularity lines $p_1^{\Phi_a}(\eta)$,$p_1^{\Phi_b}(\eta)$,$p_2^{\Phi_b}(\eta)$ and $p_1^{\Phi_c}(\eta)$. In particular the extra singularity lines $p_1^{\Phi_a}(\eta)$,$p_2^{\Phi_b}(\eta)$ and $p_1^{\Phi_c}(\eta)$ yield spectral singularities in w plane respectively that pass through points $w = -2\Phi_a + \pi/2$, $w = -4\Phi_b + \pi/2$ and $w = -2\Phi_c + \pi/2$, if not treated with correction terms. The correction terms are computed as reported in (35) and using the indications of Sections IV-A and V and [55]. A deep study of singularity lines in general needs their graphic representation

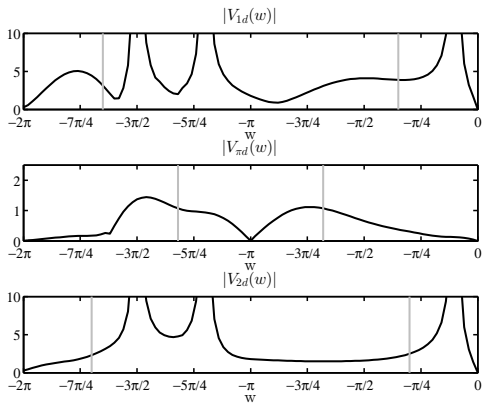

Fig. 7: Test Case. Plots of $|V_{1d}(w)|, |V_{1\pi d}(w)|, |V_{2d}(w)|$ of the reference solution (integration parameters $A = 40, h = 0.1$) in $-2\pi < w < 0$. Gray bars represent the limits useful for GTD computation, i.e. $-\pi - \Phi_f < w < -\pi + \Phi_f$, $f = a, b, c$. Peaks are observed in correspondence of GO poles.

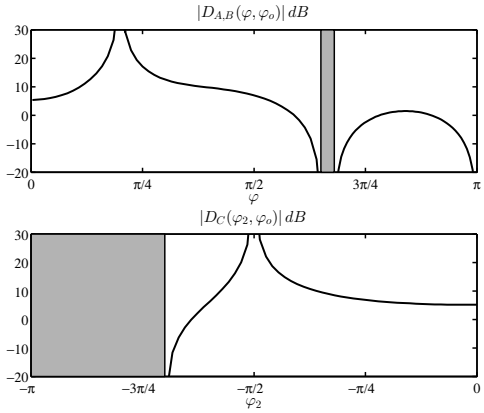

Fig. 8: Test Case. Plots of GTD diffraction coefficient in dB scale. Top: regions A and B. Bottom: region C. Peaks occur for caustics of GO (GO shadow boundaries).

together with integration lines used to derive and solve the FIEs. Similar considerations hold using the Norton model of angular regions to compute $\mathbf{I}_+(\eta)$. The same property does not occur in the Norton model of the layer region because of the absence of singularity lines. Once obtained the spectra in $-\pi < Re[w] < 0$ the application of recursive equations (93) allow to obtain the spectra for any w.

To check the convergence we select several sets of integration parameters A and h for the solution of (86). In Fig. 6 we illustrate the convergence of the axial spectral voltages in the segment $-\pi < w < 0$ before the application of recursive equations. For each spectral component and selection of integration parameters we have estimated the relative error in log_{10} scale with respect to the reference solution $A = 40$, $h = 0.1$. The plotted numerical results demonstrate the convergence at least for $A = 30$, $h = 0.2$.

In Fig. 7 we show the spectra of the three voltage unknowns reconstructed in $-2\pi < w < 0$ using the recursive equations for the reference solution. The figure shows in gray bars the w-limits useful for GTD computation. Peaks of the spectra are observed in correspondence of GO poles, i.e. incident wave $w_o = -\varphi_o = -0.1\pi$, face A reflected wave $w_{RA} = -2\Phi_a + \varphi_o = -1.2\pi$, face C reflected wave $w_{RC} = -2\Phi_c - \varphi_o = -1.5\pi$.

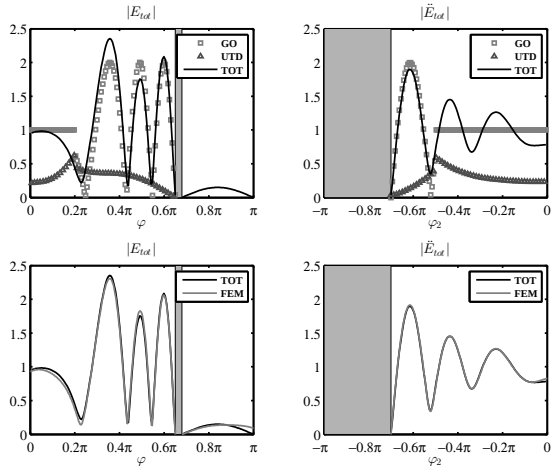

Fig. 9: Test Case. Top-left: total far field at $k\rho = 10$ for region A+B with respect to the origin O (Fig. 1) and its composition in terms of GO and UTD components for the reference solution (integration parameters $A = 40, h = 0.1$). Top-left: total far field at $k\rho_2 = 10$ for region C with respect to the origin O'' (Fig. 1) and its composition in terms of GO and UTD components for the reference solution. Bottom: corresponding comparisons with the FEM solution as described in main text.

Using (101) for Region A and (107) for Region B and extrapolating an analogous expression for for Region C (starting from Region A) we compute GTD diffraction coefficients. Fig. 8 shows the GTD diffraction coefficients in dB scale for the problem under examination. Peaks occur for caustics of GO (GO shadow boundaries), i.e. face A reflected wave $\varphi_{RA} = -\pi - w_{RA} = 0.2\pi$ and face C reflected wave $\varphi_{RC} = \pi + w_{RC} = -0.5\pi$.

Fig. 9 shows on the top-left the total far field in regions A and B at $k\rho = 10$ with respect to the origin O (Fig. 1) and its composition in terms of GO and UTD components for the reference solution. In the same figure on the bottom-left side we have reported the comparison between the solution proposed in this paper and the FEM solution taken as reference for comparison (see description at the beginning of this Section for details) in terms of total far-field at $k\rho = 10$.

Fig. 9 shows on the top-right the total far field in region C at $k\rho_2 = 10$ with respect to the origin O'' (see Fig. 1 and notation in the Introduction) and its composition in terms of GO and UTD components for the reference solution. In the same figure on the bottom-right side we have reported the comparison between the solution proposed in this paper and the FEM solution in terms of total far-field at $k\rho_2 = 10$.

From bottom of Fig. 9 we observe a good agreement between the FEM solution and the proposed solution except for $\varphi = \pi$ and $\varphi_2 = 0$. This small discrepancy is due to the application of saddle point technique for the approximation of GTD field while the saddle point is near the branch point $\eta = +k$. Improvements of asymptotics are out of the scope of this paper, however solution for this kind of approximation are reported in [58]. Finally to further validate the solution Fig. 10 presents a self-convergence study of the relative error of total field with respect to the reference solution ($A = 40, h = 0.1$) in terms of integration parameters A, h.

As stated at the beginning of this Section, according to

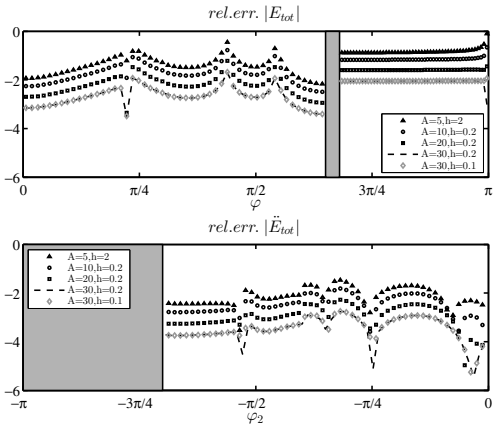

Fig. 10: Test Case. Top, Bottom: respectively relative error in log_{10} scale of total far field for region A+B at $k\rho = 10$ and C at $k\rho_2 = 10$ with respect to the reference solution in terms of integration parameters A, h.

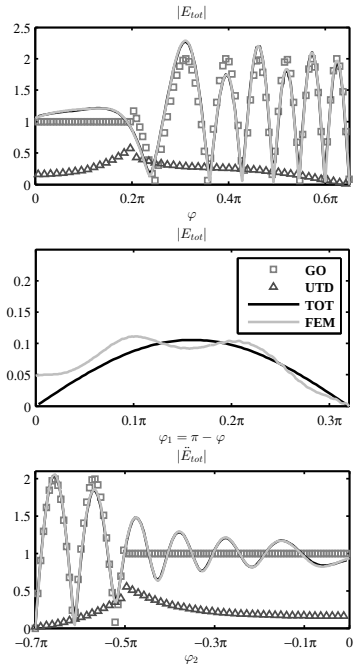

Fig. 11: Test Case. Top, Center, Bottom: respectively total far field at $k\rho = 20$ for region A+B and at $k\rho_2 = 20$ for region C. Legend is reported in the center for all the three sub-figures.

our opinion we assert and demonstrate the superiority of the proposed semi-analytical technique for infinite canonical problems. Fig. 11 shows the comparison between the solution proposed in this paper and the FEM solution in terms of total far-field at $k\rho = 20$ for region A+B and at $k\rho_2 = 20$ for region C. In this case we observe that, despite the facts that the truncation of the geometry is quite far (at 12λ) and refinement with quadratic triangular mesh is used (max side less than $\lambda/10$), we observe spurious non physical oscillations for FEM solution at $k\rho = 20$ in region B that degenerate at further distance.

VIII. Conclusions

In this paper, we present a new method to study the scattering of a plane electromagnetic wave by two separated arbitrarily oriented perfectly electrically conducting (PEC) wedges with parallel axes. The problem is formulated in a unique entire model based on GWHEs with the help of network interpretations that takes into consideration the true near-field interaction of the two wedges avoiding multiple steps of interaction among separated objects. The proposed method allows to accurately predict the effect of double PEC wedge problem useful in the computation of path loss in propagation with diffraction phenomena.

The numerical results are presented in terms of GTD/UTD diffraction coefficients and total far fields for engineering and physical applications such as propagation, radar technologies, antenna technologies, electromagnetic compatibility, electromagnetic shielding, security scan and wireless communication.

Acknowledgment

This work was partially supported by Politecnico di Torino and the Istituto Superiore Mario Boella (ISMB), Torino, Italy.

References

[1] H. Poincare', "Sur la polarization par diffraction," *Acta Math.,* vol. 16, pp. 297-339, 1892.

[2] A. Sommerfeld, "Mathematische theorie der diffraktion," *Math. Ann.,* vol. 47, pp. 317-341, 1896.

[3] H.M. MacDonald, "A class of diffraction problems," *Proc. London Math. Soc.,* vol. 14, pp. 419-427, 1915.

[4] G.D. Maliunizhets,"Inversion formula for the Sommerfeld Integral," *Sov.Phys. Dokl.,* vol. 3, pp. 52-56, 1958.

[5] G.D.Maliuzhinets, "Excitation, reflection and emission of surface waves from a wedge with given face impedance," *Soviet Phys. Dokl.,* vol. 3, pp. 752-755, 1958.

[6] B. Budaev, *Diffraction by wedges,* London, UK: Longman Scient., 1995.

[7] T.B.A. Senior, and J.L. Volakis, *Approximate boundary conditions in electromagnetics,* London, UK: IEE, 1995.

[8] J. M. L. Bernard, "Diffraction at skew incidence by an anisotropic impedance wedge in electromagnetism theory: A new class of canonical cases," *J. Physics A: Math. Gen.,* vol. 31, no. 2, pp. 595-613, 1998.

[9] V.M. Babich, M.A. Lyalinov, and V.E. Grikurov, *Sommerfeld-Malyuzhinets Technique in Diffraction Theory,* Oxford, UK: Alpha Science, 2007.

[10] D.S. Jones, *The theory of electromagnetism,* Oxford, UK: Pergamon Press, 1964.

[11] A.V. Osipov, "On the method of Kontorovich-Lebedev integrals in problems of wave diffraction in sectorial media," in *Problems of diffraction and propagation of waves*, Vol. 25, pp. 173-219, St Petersburg University Publications, 1993.

[12] A.D. Rawlins, "Diffraction by, or diffusion into, a penetrable wedge," *Proc. Royal Society Math., Phys. Engrng. Sci.,* 455, pp.2655-2686, 1999.

[13] M.A. Salem, A. Kamel, and A.V. Osipov, "Electromagnetic fields in the presence of an infinite dielectric wedge," *Proc. Royal Society Math., Phys. Engrng. Sci.,* vol. 462, pp. 2503-2522, 2006.

[14] V. Daniele, "The Wiener-Hopf technique for impenetrable wedges having arbitrary aperture angle," *SIAM Journal of Applied Mathematics,* vol.63, n.4, pp. 1442-1460, 2003.

[15] V.G. Daniele and G. Lombardi, "The Wiener-Hopf technique for impenetrable wedge problems," in Proc. of Days on Diffraction Internat. Conf., invited paper, pp. 50-61, Saint Petersburg, Russia, June 2005.

[16] V. Daniele, and G. Lombardi, "Wiener-Hopf Solution for Impenetrable Wedges at Skew Incidence," *IEEE Trans. Antennas Propagat.,* vol. 54, n. 9, pp. 2472-2485, Sept. 2006.

[17] V. Daniele, "The Wiener-Hopf formulation of the dielectric wedge problem: Part I," *Electromagnetics*, vol. 30, n. 8, pp. 625-643, 2010.

[18] V. Daniele, "The Wiener-Hopf formulation of the dielectric wedge problem: Part II," *Electromagnetics*, vol. 31, n. 1, pp. 1-17, 2011.

[19] V. Daniele, "The Wiener-Hopf formulation of the dielectric wedge problem. Part III: The skew incidence case," *Electromagnetics*, vol. 31, n. 8, pp. 550-570, 2011.

[20] V. Daniele, and G. Lombardi, "The Wiener-Hopf Solution of the Isotropic Penetrable Wedge Problem: Diffraction and Total Field," *IEEE Trans. Antennas Propagat.,* vol. 59, n. 10, pp. 3797-3818, Oct. 2011.

[21] G. Lombardi, "Skew Incidence on Concave Wedge With Anisotropic Surface Impedance," *IEEE Antennas Wireless Propag. Lett.,* vol. 11, pp. 1141-1145, 2012

[22] V.G.Daniele, and G.Lombardi,"Fredholm Factorization of Wiener-Hopf scalar and matrix kernels," *Radio Science,* vol. 42,RS6S01,pp.1-19, 2007

[23] V. Daniele, R. Zich, *The Wiener-Hopf method in electromagnetics,* Raleigh, NC: SciTech Publishing, 2014

[24] B.Noble,*Methods Based on the Wiener-Hopf Technique: For the Solution of Partial Differential Equations,*London,UK:Pergamon, 1958.

[25] L.A. Weinstein, *The Theory of Diffraction and the Factorization Method,* Boulder, Colorado: The Golem Press, 1969.

[26] R. Mittra, S.W. Lee, *Analytical Techniques in the Theory of Guided Waves,* New York: The MacMillan Company, 1971.

[27] J.B. Lawrie, I.D. Abrahams, "A brief historical perspective of the Wiener-Hopf technique," *Journal of Engineering Mathematics,*, vol. 59, n.4, pp. 351-358, 2007.

[28] K. Aoki, K. Uchida, "Scattering of plane electromagnetic waves by a conducting rectangular cylinder-E polarized wave," *Mem.Fac. Eng. Kyushu Univ.,* vol. 38, pp. 153-175, 1978.

[29] K. Aoki, A. Ishizu, K. Uchida, "Scattering of surface waves in Semi-infinite slab dielectric guide," *Mem.Fac. Eng. Kyushu Univ.,* vol. 42, pp. 197-215, 1982.

[30] M. Idemen, L. B. Felsen, "Diffraction of a Whispering Gallery Mode by the Edge of a Thin Concave Cylindrically Curved Surface," *IEEE Trans. Antennas Propag,* vol. AP-29, no. 4, pp. 571-579, 1981.

[31] E. Luneberg and R. A. Hurd, "On the diffraction problem of a half plane with different face impedances," *Can. A. Phys.,* vol.62, pp.853-860, 1984.

[32] R.A.Hurd, S.Przezdziecki, "Half-plane diffraction in a gyrotropic medium," *IEEE Trans. Antennas Propag.,* vol.33, pp. 813-822, Aug 1985

[33] I.D. Abrahams, G.R. Wickham, "On the scattering of sound by two semi-infinite parallel staggered plates. I. Explicit matrix Wiener-Hopf factorization," *Proc. Royal Soc. London*, vol. A420, pp. 131-155, 1988.

[34] I.D. Abrahams , G.R. Wickham, "General Wiener-Hopf factorization of matrix kernel with exponential phase factors," *SIAM J. Appl. Math.,* vol.50, n.3, pp. 819-838, 1990.

[35] A. Buyukaksoy, A.H Serbest, "Matrix Wiener-Hopf Factorization Methods and Applications to Some Diffraction Problems," ch.6 in *Analytical and Numerical Methods in Electromagnetic Wave Theory,* M. Hashimoto, M.Idemen and O.A. Tretyakov Editors, Tokio, Japan: Science House Co.,Ltd., pp. 257-315, 1993.

[36] K. Kobayashi, "Some Diffraction problems involving modified Wiener-Hopf geometries," in M. Hashimoto, M. Idemen and O.A. Tretyakov (editors), *Analytical and Numerical Methods in Electromagnetic Wave Theory,* Tokio, Japan: Science House Co.,Ltd., pp.147-228, 1993.

[37] E. Luneburg, A.H. Serbest, "Diffraction of a obliquely incident plane wave by a two-face impedance half plane: Wiener-Hopf approach," *Radio Science,* vol. 35, pp. 1361-1374, 2000.

[38] E. Topsakal, A. Buyukaksoy, M. Idemen, "Scattering of electromagnetic waves by a rectangular impedance cylinder," *Wave Motion,* vo. 31, pp.273-296, 2000.

[39] A. Buyukaksoy, G. Uzgoren and F. Birbir, "The scattering of a plane wave by two parallel semi-infinite overlapping screens with dielectric loading," *Wave Motion,* vol. 34, pp.375-389, 2001.

[40] I.H. Tayyar, A. Buyukaksoy, "Plane wave diffraction by two oppositely placed, parallel two part planes," *IEE Proc.-Sci. Meas. Technol.,* vol. 153, pp 169-176, 2003.

[41] G. Cinar, A. Buyukaksoy, "Diffraction on a normally incident plane wave by three parallel half-planes with different face impedances," *IEEE Trans. Antennas Propag.,* vol. 52, pp.478-486, 2004.

[42] Y.A. Antipov, V.V. Silvestrov, "Electromagnetic scattering from an anisotropic half-plane at oblique incidence: the exact solution," *Quart. J. Mech. Appl. Math.,* vol. 59, 211-251, 2006.

[43] N.Tymis,I.Thompson,"Low-frequency scattering by a semi-infinite lattice of cylinders,"*Quart J Mech Appl Math,* vol 64,n 2,pp 171-195,2011

[44] A.D. Rawlins, "The method of finite-product extraction and an application to Wiener-Hopf theory," *IMA J. Appl. Math.,* vol 77, n.4, pp. 590-602, 2012.

[45] R. Nawaz, M. Ayub, "An exact and asymptotic analysis of a diffraction problem,", *Meccanica,* vol. 48, n. 3, pp. 653-662, 2013.

[46] R .Nawaz, A. Naeem, M. Ayub, A. Javaid, "Point source diffraction by a slit in a moving fluid," *Waves in Random and Complex Media,* vol. 24, n. 4, pp. 357-375, 2014.

[47] D.G. Crowdy, E. Luca, "Solving Wiener-Hopf problems without kernel factorization," *Proc. R. Soc. Lond. Ser. A Math. Phys. Eng. Sci.,* vol. 470, n. 2170, art. no. 20140304, 20 pp. 2014.

[48] M. Ayub, T.A. Khan, K. Jilani, "Effect of cold plasma permittivity on the radiation of the dominant TEM-wave by an impedance loaded parallel-plate waveguide radiator,", *Mathematical Methods in the Applied Sciences,* vol. 39, n. 1, pp. 134-143, 2016.

[49] S. Rogosin, G. Mishuris, "Constructive methods for factorization of matrix-functions," *IMA J. Appl. Math.,* vol.81, n. 2, pp. 365-391, 2016.

[50] G. Fusai, G. Germano, D. Marazzina,"Spitzer identity, Wiener-Hopf factorization and pricing of discretely monitored exotic options," *European Journal of Operational Research,* vol. 251, n.1, pp. 124-134, 2016.

[51] D. Margetis, M. Maier, M. Luskin, "On the Wiener-Hopf Method for Surface Plasmons: Diffraction from Semiinfinite Metamaterial Sheet," *Studies in Applied Mathematics,* vol. 139, n. 4, pp. 599-625, 2017.

[52] A. Kisil, L.J. Ayton, "Aerodynamic noise from rigid trailing edges with finite porous extensions," *J Fluid Mech,* vol. 836, pp. 117-144, 2018.

[53] V.G. Daniele, "Electromagnetic fields for PEC wedge over stratified media. Part I," *Electromagnetics*, vol. 33, pp. 179-200, 2013.

[54] V.G. Daniele, G. Lombardi, "Arbitrarily oriented perfectly conducting wedge over a dielectric half-space: diffraction and total far field," *IEEE Trans. Antennas Propag.,* vol. 64, n. 4, pp. 1416-1433, 2016.

[55] V.G. Daniele, G. Lombardi, R.S. Zich, "Network representations of angular regions for electromagnetic scattering," *Plos One,* vol. 12, n. 8, e0182763, pp. 1-53, 2017, https://doi.org/10.1371/journal.pone.0182763.

[56] V.G. Daniele, G. Lombardi, R.S. Zich, "The electromagnetic field for a PEC wedge over a grounded dielectric slab: 1. Formulation and validation," *Radio Science,* vol. 52: 2017RS006355, pp. 1-20, 2017.

[57] V.G. Daniele, G. Lombardi, R.S. Zich, "The electromagnetic field for a PEC wedge over a grounded dielectric slab: 2. Diffraction, Modal Field, SurfaceWaves, and Leaky Waves," *Radio Science,* vol. 52, pp. 1-18, 2017.

[58] L. B. Felsen and N. Marcuvitz, *Radiation and Scattering of Waves,* Englewood Cliffs, NJ: Prentice-Hall, 1973.

[59] V.G. Daniele, R.D. Graglia, G. Lombardi, P.L.E. Uslenghi, "Cylindrical resonator sectorally filled with DNG metamaterial and excited by a line source," *IEEE Antennas Wireless Propag. Lett.,* vol. 11, pp. 1060-1063, 2012.

[60] V.G. Daniele, Diffraction by two wedges, Report DET-2014-1, 2014, http://personal.delen.polito.it/vito.daniele

[61] V. G. Daniele, R. S. Zich, "Diffraction by two wedges," in Proc. IEEE AP-S Int. Symp., Vancouver, BC, 2015, pp. 1380-1381.

[62] V. Daniele, G. Lombardi, R.S. Zich, "Analysis of coupled angular regions in spectral domain," URSI International Symposium on Electromagnetic Theory, EMTS 2016, pp. 73-75.

[63] V. G. Daniele, G. Lombardi and R. S. Zich, "On circuital modelling of diffraction problems in spectral domain," in Proc. IEEE AP-S Int. Symp., San Diego, CA, 2017, pp. 39-40.

[64] H. Nussenzveig, "Solution of a diffraction problem I. The Wide Double Wedge," *Phil. Trans. R. Soc. Lond. A*, vol. 252, pp. 1-30, 1959.

[65] H. Nussenzveig, "Solution of a diffraction problem II. The Narrow Double Wedge," *Phil. Trans. R. Soc. Lond. A*, vol. 252, pp. 31-51, 1959.

[66] B. Teague, N. Zitron, "Diffraction by an aperture between two wedges," *Appl. Sci. Res.*, vol. 26, pp. 127-137, 1972.

[67] S.Lee, L.Grun,"Radiation from flanged waveguide: comparison of solutions," *IEEE Trans Antennas Propagat*, vol.30, no.1, pp.147-148,1982

[68] R. Tiberio, R.G. Kouyoumjian, "An Analysis of Diffraction at Edges, Illuminated by Transition Region Fields," *Radio Science,* Vol. 17, pp. 323-336, 1982.

[69] A. Elsherbeni, M. Hamid, "Diffraction by a wide double wedge," *IEEE Trans. Antennas Propag.,* vol. 32, no. 11, pp. 1262-1265, 1984.

[70] H.H. Syed, J.L. Volakis, "Multiple diffractions among polygonal impedance cylinders," *IEEE Trans. Antennas Propag.,* vol. 37, no. 5, pp. 664-672, 1989.

[71] R.Tiberio, G.Manara, G. Pelosi and R.G.Kouyuoumjian, "High-frequency electromagnetic scattering of plane waves from double wedges," *IEEE Trans Antennas Propag,* vol. 37, no. 9, pp. 1172-1180, 1989.

[72] M.Schneider,R.J.Luebbers,"A general, uniform double wedge diffraction coefficient,"*IEEE Trans Antennas Propag,*vol. 39,n. 1,pp. 8-14,1991

[73] L.P.Ivrissimtzis, R.J.Marhefka, "Double diffraction at a coplanar skewed edge configuration,"*Radio Science,* vol 26, n 4, pp. 821-830, 1991

[74] D. Erricolo and L. E. Uslenghi, "Two-dimensional simulator for propagation in urban environments," *IEEE Trans. on Vehicular Technology,* vol. 50, no. 4, pp. 1158-1168, 2001.

[75] M. Albani, "A uniform double diffraction coefficient for a pair of wedges in arbitrary configuration," *IEEE Trans. Antennas Propag.,* vol. 53, no. 2, pp. 702-710, 2005.

[76] J.M.L. Bernard, "A spectral approach for scattering by impedance polygons," *Quart J Mech Appl Math,* Vol 59, n 4, pp 517-550, 2006

[77] A. Toccafondi, R. Tiberio, "An incremental theory of double edge diffraction," *Radio Science,* vol 42, RS6S30, pp. 1-13, 2007.
[78] G. Carluccio, M. Albani, "An Efficient Ray Tracing Algorithm for Multiple Straight Wedge Diffraction," *IEEE Trans. Antennas Propag.,* vol. 56, no. 11, pp. 3534-3542, 2008.
[79] A. Toccafondi, S.M. Canta, D. Erricolo, "ITD Double-Edge Diffraction for Complex Source Beam Illumination," *IEEE Trans. Antennas Propag.,* vol. 61, no. 5, pp. 2688-2694, 2013.
[80] T. Negishi et al., "Measurements to Validate the UTD Triple Diffraction Coefficient," *IEEE Trans. Antennas Propag.,* vol. 62, no. 7, pp. 3723-3730, 2014.
[81] M.A. Lyalinov, "Integral Equations and the Scattering Diagram in the Problem of Diffraction by Two Shifted Contacting Wedges with Polygonal Boundary," *J. Math. Sci.,* vol. 214, n. 3, pp. 322-336, 2016.
[82] R.D. Graglia and G. Lombardi, "Singular higher order complete vector bases for finite methods," *IEEE Trans. Antennas Propag.,* vol. 52, no. 7, pp. 1672-1685, Jul. 2004.
[83] R. D. Graglia, G. Lombardi, D. R. Wilton and W. A. Johnson, "Modeling edge singularities in the method of moments," 2005 IEEE Antennas and Propagation Society International Symposium, Washington, DC, 2005, pp. 56-59 vol. 3A.
[84] R. D. Graglia and G. Lombardi, "Singular higher order divergence-conforming bases of additive kind and moments method applications to 3D sharp-wedge structures," *IEEE Trans. Antennas Propag.,* vol. 56, no. 12, pp. 3768-3788, Dec. 2008.
[85] F. Gakhov, *Boundary value problems,* Ch. 9, Dover Publications, 1990
[86] V.G. Daniele, G. Lombardi, R.S. Zich, "The scattering of electromagnetic waves by two opposite staggered perfectly electrically conducting half-planes," *Wave Motion, in press,* Oct. 2018, doi: 10.1016/j.wavemoti.2018.09.017
[87] L.V. Kantorovich and V.I. Krylov, *Approximate methods of higher analysis,* Groningen, The Netherlands: Noordhoff, 1964.
[88] J. van Bladel, *Singular Electromagnetic Fields and Sources,* Oxford, UK: Clarendon, 1991.
[89] V.G. Daniele, "Rotating Waves in the Laplace Domain for Angular Regions," *Electromagnetics,*, vol. 23, n. 3, pp. 223-236, 2003.
[90] R. G. Kouyoumjian and P. H. Pathak, "A uniform geometrical theory of diffraction for an edge in a perfectly conducting surface," *Proc. IEEE,* vol. 62, pp. 1448-1461, Nov. 1974.

Vito Daniele was born in Catanzaro, Italy, on March 20, 1942. He received the degree in electronic engineering from Polytechnic of Turin, Italy, in 1966. In 1980, he was appointed Full Professor in Electrical Engineering at the University of Catania. From 1981 to 2012 he was Professor of Electrical Engineering at the Polytechnic of Turin and since 2015 he is Emeritus Professor at the same Polytechnic.

He has served also as a Consultant to various industries in Italy. He has published more than 150 papers in refereed journals and conference proceedings and several textbook chapters.

His research interests are mainly in analytical and approximate techniques for the evaluation of electromagnetic fields both in high and in low frequency. In particular his studies on the Wiener Hopf technique have produced the recent book "The Wiener-Hopf Method in Electromagnetics". Prof. Daniele was the Guest Editor of a special issue on Electromagnetic Coupling to Transmission Lines for Electromagnetics in 1988, Chairman and Invited Speaker for several international symposia, and reviewer for many international journals.

Since 2013 he is corresponding Member of the Academy of Sciences of Torino.

Guido Lombardi (S'02-M'03-SM'11-) was born in Florence, Italy, on December 8, 1974. He received the Laurea degree (*summa cum laude*) in telecommunications engineering from the University of Florence, Italy, in 1999 and the Ph.D. degree in electronics engineering at the Polytechnic of Turin, Italy, in jan. 2004. In 2000-01, he was officer of the Italian Air Force. In 2004 he was an Associate Researcher with the Department of Electronics of Polytechnic of Turin and in 2005 he joined the same Department as an Assistant Professor with tenure and where he is currently an Associate Professor. He was the recipient of the Raj Mittra Travel rant award for junior researcher at 2003 IEEE AP-S International Symposium and USNC/CNC/URSI National Radio Science Meeting, Columbus, OH, USA. In the same year he was Visiting Researcher at the Department of Electrical and Computer Engineering, University of Houston, Houston, TX, USA. In 2018 he was recipient of the London Mathematical Society Research in Pairs grant as research visitor to the University of Cambridge, UK. His research interests comprise analytical and numerical methods for electromagnetics, Wiener-Hopf method, diffraction, theoretical and computational aspects of FEM and MoM, numerical integration, electromagnetic singularities, waveguide problems, microwave passive components, project of orthomode transducers (OMT), metamaterials. He is an associate editor of the IEEE ACCESS journal, the IEEE Trans. Antennas Propagat and the IET Electronics Letters. He is an IEEE APS AdCom member for the triennium (2016-18) and (2019-21). He served as member of the Organizing Committee in the International Conference on Electromagnetics in Advanced Applications (ICEAA) since the 2001 edition and in the IEEE-APS Topical Conference on Antennas and Propagation in Wireless Communications (IEEE-APWC) since the 2011 edition. He was Publication Chair of ICEAA and IEEE-APWC since 2011 edition. He served the 2012 and 2015 IEEE AP-S International Symposium and USNC/CNC/URSI National Radio Science Meeting, Chicago, IL, USA as co-organizer of the Special Sessions on innovative analytical and numerical techniques for complex scattering problems, special materials, nanostructures. He regularly serves as a reviewer of several international journals on physics, electrical engineering and electromagnetics, among which IEEE, IET, Wiley, Elsevier, PLoS, ACES Journals and Transactions.

Rodolfo S. Zich (Honorary Member '16-)was born in Torino, Italy, on July 15, 1939. He graduated in Electronic Engineering at Politecnico di Torino in 1962, where he has been full professor of Electromagnetic Fields and Circuits since 1976; now Emeritus (2010). He served as Rector of Politecnico from 1987 to 2001.

He has an extensive international experience: he was member of the Board of Directors of Ecole Polytechnique de Paris (Palaiseau); President of Columbus (Association of Latin America and Europe Universities) and CLUSTER (Cooperative Link between Universities for Science, Technology for Education and Research). Very active in promoting education and applied research in cooperation with public and private partners; in 1999 he founded Istituto Superiore Mario Boella, a research center on Information and Communication Technologies (ICT).

Author of several papers, his scientific interests are mainly on hybrid analytical functional techniques in electromagnetic scattering. Gold Medal and First Class Diploma of Merit for Science, Culture and Art (2007, Italy); member of the National Academy of Science of Turin (2001).

He was awarded the IEEE Honorary membership in 2016.